Carbonate Chemistry in the San Juan Channel: Characterization and Suggestions for Mitigation

Constance Amanda Sullivan

A thesis

submitted in partial fulfillment of the

requirements for the degree of

Master of Marine Affairs

University of Washington

2012

Committee:

Terrie Klinger

Jan Newton

Thomas Leschine

Program Authorized to Offer Degree:

School of Marine and Environmental Affairs

University of Washington

Abstract

Carbonate Chemistry in the San Juan Channel: Measurements and Mitigation

Constance Amanda Sullivan

Chair of the Supervisory Committee:

Terrie Klinger

School of Marine and Environmental Affairs

Recent attention has been given to the potential vulnerability of coastal zones to ocean acidification. Urban estuaries such as the Salish Sea are strongly influenced by human activities and could be particularly vulnerable to the added stress of ocean acidification. At the same time, very little is known about ocean acidification condition in urban estuaries. To begin to address this need, I sampled seawater and measured carbonate chemistry at two stations and four depths over seven sampling time points during the fall of 2011. pH was variable but in all samples was substantially lower than contemporary values in open-ocean settings. pCO_2 was correspondingly high. Aragonite saturation state – a

measure of the kinetics of calcium carbonate precipitation – was uniformly undersaturated. Compared to open oceanic values, the relatively wide range in variation of carbonate variables observed could be due to a diversity of influences in this estuarine area, including the intrusion of upwelled waters from the outer coast, local upwelling within the Salish Sea, discharge from rivers, and inputs from human activities other than fossil fuel combustion. This last class of stressors – those that result from regional human activities – can be managed as a transboundary pollution issue. I propose that a regulatory toolkit be developed for use by regulators in the U.S. and Canada to address transboundary pollution issues under existing agreements. The toolkit will allow regulators to ascertain the extent of point-source discharges that can add regional ocean acidification and to develop local mitigation strategies to reduce the negative impacts of OA in the Salish Sea.

Table of Contents

List of Figures

List of Tables

Acknowledgements

I would like to thank my committee for all of your support during the past 2 years. To my advisor, Terrie Klinger, thank you for all of your guidance and for always being around to help out. Thanks especially for helping me to find the perfect project. To Jan Newton, it has been so much fun to transition from an undergrad student to grad student to colleague with you over the past 10 years. Thank you for all of your guidance and pep talks. To Tom Leschine, thank you for helping me to learn how to put science to use in the policy and management context and for providing valuable academic and career advice.

This project could not have been possible without the support from so many other people. A huge thanks to Moose O'Donnell for training me on the OA lab and for all of the time you took to help me out with the design, execution, and analysis of my project. Thanks to Breck Tyler and Eric Anderson for hiring me so many times to work at my favorite place, the University of Washington's Friday Harbor Laboratories, so that I would have the opportunity to pursue my thesis work. To the 2011 Friday Harbor Pelagic Ecosystem Function Research Apprenticeship (especially the oceanography crew!), thanks for helping me take samples and for bringing me food and hugs on long lab days. Wolf Krieger and Dennis Willows generously donated their time to drive the *Centennial* on the cruises that my samples were collected on. Simone Alin (PMEL, NOAA) was invaluable in the analysis of these data. Steve Emerson (Oceanography, UW) was very helpful in some of the calculations for this project and was a valuable source to bounce ideas off of.

The sampling cruises that facilitated my thesis research were conducted as part of the University of Washington's Pelagic Ecosystem Function Research Apprenticeship (Newton and Tyler) in which I was a Research Assistant during Fall 2011. Funds for the carbonate chemistry sample analysis came from a small grant to Newton by the UW College of the Environment.

To the gang in Friday Harbor, thanks for all the great times and for letting me crash on so many floors and couches. You guys are the best and are the most fun support system. Thanks also to my buds at SMEA: you guys are amazing and made the process of obtaining this degree enjoyable.

Finally, a heartfelt thank you to my parents, brother, grandma, aunt, and uncle: thank you for the support, love, guidance, and for being the incredible people you all are. I would not be who or where I am without you.

Chapter One: Measurements

Introduction

Estuaries are vital to the ecological and social systems that surround them (Huppert et al. 2003). They often are highly productive, providing food for wildlife and humans, habitat for economically valuable organisms such as salmon (Simenstead and Cordell 2000) and bivalves (Dumbauld et al. 2009), and additional ecosystem services that in combination make estuaries highly desirable areas for human habitation. As a consequence, many estuaries have been heavily urbanized. Puget Sound in Washington State, which is part of the Salish Sea, is one such example of an urbanized estuarine system.

The condition of waters in urban estuaries is influenced by: 1) the proportion and condition of waters coming from fluvial and oceanic sources; 2) physical processes such as circulation and mixing; 3) biological processes such as photosynthesis and respiration; and 4) human-induced changes to marine biogeochemical cycles through the addition of toxins, pollutants, and other material from marine, terrestrial, and atmospheric sources, habitat loss and modification, and removals of biomass via fishing.

Coastal waters are naturally low in pH (Doney 2010), and in the last 30 years, the average pH of coastal waters globally has declined by 0.02 units per decade

(Hoegh-Guldberg and Bruno 2010). Such rapid changes in pH can exceed the buffering capacity of the system (Caldeira and Wickett 2003).

Reductions in pH that result from anthropogenic activity are known as ocean acidification (Feely et al. 2009). The oceans act as a sink for atmospheric carbon, and have absorbed approximately one-third of the atmospheric carbon dioxide produced since the Industrial Revolution (Hoegh-Guldberg and Bruno 2010). When carbon dioxide is added to seawater, the pH is driven down, and the saturation states of the calcium carbonate ions calcite and aragonite are reduced (Feely et al. 2009).

The saturation state of an ion (Ω) is determined by temperature, salinity, and pressure (Logan 2010). Thermodynamically, when the saturation state for either carbonate ion is less than 1, the conditions are referred to as undersaturated and dissolution of carbonate structures can occur. When the saturation state equals 1, there is an equal chance of dissolution or precipitation, and when it is above 1, the conditions are considered oversaturated and precipitation can occur. Biological systems can modify these thermodynamic constraints, but saturation states of 1 or less are considered to be corrosive to shells and skeletons. Surface waters of the ocean are typically supersaturated with respect to calcite and aragonite (Doney 2010); however, as anthropogenic CO_2 is added to the ocean, saturation levels appear to be declining and saturation horizons shoaling.

In the eastern Pacific Ocean along the coast of western North America, a seasonal upwelling regime begins early in spring and lasts until late fall (Feely et al. 2008; Davenne and Masson 2001). This seasonal upwelling brings deeper waters that are relatively lower in pH and enriched in pCO_2 to the surface and causes the calcium carbonate saturation horizon to shoal (Feely et al. 2008). The pH levels on the west coast of North America vary over space and time (Hofmann et al. 2011), in part due to variability in the strength of coastal upwelling (Feely et al. 2008).

Factors other than upwelling can influence carbonate chemistry in coastal areas. River waters tend to be lower in pH than ocean waters (Salisbury et al. 2008) and consequently can reduce seawater pH in coastal areas. Pollutants released to coastal waters from point sources such as wastewater treatment plants, pulp and paper mills, mine effluents, and concentrated feedlot areas can contribute to localized changes in seawater chemistry (Kelly and Caldwell 2012), as can pollutants from non-point sources such as runoff from agricultural areas and impervious surfaces (Kelly and Caldwell 2012; Doney et al. 2007). Releases of sulfur (SO_X) and nitrogen (NO_X) oxide compounds to the atmosphere, for example, from industrial and shipping activities, can cause the formation of acids in aquatic environments (Doney et al. 2009), thereby influencing seawater carbonate chemistry.

Relatively few studies have described the natural variation in carbonate chemistry along the coast of western North America (Hofmann et al. 2011; Feely et al. 2010; Hales et al. 2005; van Geen et al. 2000). Here I begin to characterize the condition of waters in the Salish Sea with respect to seawater carbonate chemistry. I measured two carbonate system variables (dissolved inorganic carbon and total alkalinity) and other physical variables (temperature, salinity, and dissolved oxygen) at two stations in October and November, 2011. These are among the first coherent measurements of carbonate and other variables made in this region of the Salish Sea, and as such they are intended to provide an initial description of local carbonate chemistry dynamics and variation over time and space. Measurements such as these are essential to development and evaluation of strategies for human mitigation of carbonate chemistry conditions in urban estuaries.

Materials and Methods

The San Juan Archipelago

The San Juan Archipelago (SJA) is located in the Salish Sea between the mainland of Washington State (USA) and Vancouver Island (Canada) (Figure 1). The islands lie near the boundary of the Strait of Georgia and the Strait of Juan de Fuca bordered by Haro Strait to the west and Rosario Strait to the east. A glacially-deposited sill is located south of the city of Victoria (BC, Canada) running perpendicular to the Strait of Juan de Fuca at depths of 55 – 100m (Davenne and Masson 2001). This sill influences local circulation and mixing

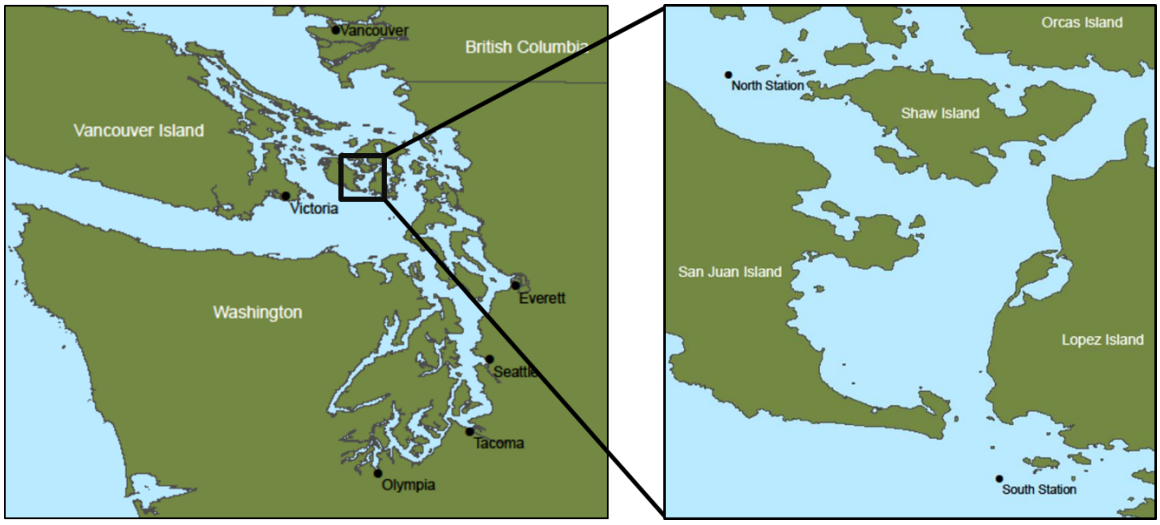

Figure 1: Map of sampling sites in San Juan Channel, San Juan Islands, Washington. North Station: 48^{O} 35.00' N, 123^{O} 02.50' W; South Station: 48^{O} 25.20' N, 122^{O} 56.60' W.

between oceanic waters from the outer coast of Washington and estuarine waters of the Salish Sea. Surrounding urban areas, including those surrounding Puget Sound (U.S.), and Victoria and Vancouver (Canada) contribute industrial and agricultural byproducts to local waters.

The oceanographic properties of these waters are well characterized (Davenne and Masson 2001). The primary river influence is from the Fraser River. Discharge from the Fraser River exhibits an annual cycle that peaks in the early summer during snowmelt from the Canadian Rockies and subsequently declines, with intermittent increases for a few days at a time at other times of the year. In the southern portion of the San Juan Archipelago, the primary influence is from the coastal waters off the coast of Washington. Coastal waters in this region are part of the northern California Current System (CCS). Waters of the CCS tend to be enriched with pCO_2 (Hauri et al. 2009) and this is especially true of water upwelled along the coast (Feely et al. 2008). Coastal waters are transported into the Salish Sea through the Strait of Juan de Fuca. Deep, dense water upwelled from the outer coast can build up behind the Victoria sill, spilling over into the boundary between the Strait of Juan de Fuca and the Strait of Georgia during the weaker of each monthly neap tide (Masson 2002). The annual upwelling and downwelling cycles in this region of the Salish Sea are wind-driven (Davenne and Masson 2001). In the summer, the winds are primarily from the northwest, creating an upwelling regime. In the winter, the winds are from the opposite

direction, causing downwelling. The transitions between these regimes are known as the fall and spring transitions.

Sampling Approach

The University of Washington's R/V *Centennial*, based out of the UW Friday Harbor Laboratories, was used for water sampling at two stations on seven days spanning a two-month period during Autumn, 2011 (Figure 1; Table 1). The North Station was located at 48º 35.00' N, 123º 02.50' W, to the west of Yellow Island. The South Station was located at 48º 25.20' N, 122º 56.60' W, to the south of Cattle Pass and at the southern entrance to the San Juan Channel. The stations are only 21km apart but have different characteristics and influencing factors. The North Station has a maximum depth of 130m, and its surface waters are seasonally influenced by discharge from the Fraser River. The South Station is located in the Strait of Juan de Fuca. It has a maximum depth of 90m and is influenced primarily by water from Puget Sound and the outer coast of Washington.

Water samples were taken from four depths at each station. At the North Station, samples were taken at 0m, 20m, 80m, and either 115m, 116m, 120m or 125m. At the South Station, samples were taken at 0m, 20m, 50m, and 80m or 85m (Table 1). At each sampling location, CTD (Sea-Bird Electronics SBE 25) casts were performed from surface to bottom to determine the salinity and temperature over depth of the water column where the samples were collected

Table 1: Sampling days in 2011 by station and depth.

Sample Date	Station	Depths Sampled (m)
7 October	North	0, 20, 80, 125
18 October	North	0, 20, 80, 120
24 October	North	0, 20, 80, 120
1 November	North	0, 20, 80, 120
7 November	North	0, 20, 80, 120
15 November	North	0, 20, 80, 115
19 November	North	0, 20, 80, 116
7 October	South	0, 20, 50, 85
18 October	South	0, 20, 50, 85
24 October	South	0, 20, 50, 85
1 November	South	0, 20, 50, 80
7 November	South	0, 20, 50, 80
15 November	South	0, 20, 50, 80
19 November	South	0, 20, 50, 80

from. All variables were calculated using Sea-Bird Electronics processing software and their annual factory calibration factors. The SBE 25 has an instrument resolution better than 0.001^{O}C for temperature and 0.001 psu for salinity. Salinity is reported as Practical Salinity.

Water samples were collected in Niskin bottles on the CTD frame during the upcast at each depth and site to determine the carbonate chemistry and dissolved oxygen concentrations.

Carbonate chemistry samples were taken in 500mL glass bottles with approximately 2 cm of headspace below the neck of the bottle. To preserve samples, 110µL of $HgCl_2$ were added to each sample. Bottles were stopped with stoppers that had been greased with Apeizon-L. Once bottles were sealed, they were inverted several times to disperse the $HgCl_2$. Samples were stored at room temperature and were analyzed within three months of collection.

Analysis of Samples

Dissolved inorganic carbon (DIC) was measured using coulometric titration. Briefly, samples were acidified with 5% phosphoric acid and purged with an inert gas using a LICOR CO_2 analyzer. CO_2 was then measured coulometrically via titration (Dickson et al. 2007). The LabWare computer program was customized for the calculation of DIC.

Each seawater sample was titrated with HCl to determine its total alkalinity (TA) (Dickson et al. 2007). The volume of HCl dispensed in the titration was used to calculate the TA. An Agilent 34970 and Metrohm Dosimat were used for the titration. The LabWare computer program was customized for the calculation of TA.

The pH, the partial pressure of CO_2 (pCO_2), and saturation states of calcite and aragonite were calculated based on measured DIC, TA, temperature, salinity, and pressure using the computer program CO_2Calc (Version 1.0).

On four cruises, replicate water samples were taken from the same Niskin from 80m at North Station. These samples were analyzed for DIC and TA and their pH and pCO_2 values calculated in CO_2Calc. The mean of the differences in calculated values of pH and pCO_2 was calculated to estimate the error propagated through the calculations based on the measured values.

Sample collection for the measurement of dissolved oxygen (DO) was performed according to the Carpenter modification of the Winkler titration method (Carpenter 1965; Winkler 1888). Briefly, samples were collected in 125mL Erlenmeyer flasks in a manner that prevented formation of air bubbles in the sample flask. One milliliter each of $MnCl_2$ and NaOH-NaI were added to the flasks prior to capping and inversion of the sample bottle. Following collection, samples were titrated to 0.001mL with Na_2SO_3 with a Beckman Dosimat

microburet. Each sample's oxygen content was calculated from the titration data. The precision of the oxygen titration values was 0.1 mg/L.

I used the temperature and salinity water mass signatures for the San Juan Archipelago of Redfield (1950) to determine the origins of water sampled at each station via the continuous measurement of the CTD (Table 2).

The calculation of the anthropogenic input of DIC was based on Feely et al. (2010). This calculation assumes that the rate of fCO_2 increase in air is the same as that in water and that adding CO_2 does not change the alkalinity of a solution. The atmospheric fCO_2 during the sampling period was based on the measured values by the NANOOS (Northwest Association of Networked Ocean Observing systems; http://www.nanoos.org) data buoy at La Push, WA (47.97°N, 124.95°W) maintained by the University of Washington and NOAA Pacific Marine Environmental Laboratory. The average value during the sampling period of this study was 346μatm, which is 66μatm higher than the preindustrial value of 280μatm. This difference was subtracted from the values of fCO_2 measured in the samples from North and South Stations. The corrected fCO_2 values and corresponding measured TA values were input into CO_2Calc to recalculate DIC. The recalculated DIC values represent the amount of DIC in the samples, minus the anthropogenic fraction. The difference between the values was calculated to estimate the amount of anthropogenic DIC in the samples in units of μmol DIC/kg SW, where SW is seawater.

Table 2. Water mass sources and their associated temperature and salinity characteristics (Redfield 1950).

Water Mass Source	**Water Temperature (^{O}C)**	**Salinity (psu)**
Surface of Strait of Georgia	10 - 11	28 - 28.6
Mix of the Strait of Juan de Fuca and the Strait of Georgia	8.5 - 11	28.6 - 30
Mix of the Strait of Juan de Fuca, the Strait of Georgia, and surface water from the Pacific Ocean	8.5 - 11	30 – 32.25
Surface of the Pacific Ocean	8.5 - 11	32.25 - 33
Mid Pacific Ocean	7.5 - 8.5	32.25 - 33

Results

North Station

Water Column Properties

The North Station was fairly well mixed over the duration of the study with respect to salinity and temperature (Figures 2 – 5). No trend over time in salinity was evident but fresher surface waters were noted on 18 Oct and 15 Nov. As the season progressed, the water became increasingly colder and the water column became increasingly well mixed with respect to temperature. Dissolved oxygen was higher at the surface than at depth for the majority of sampling days (Figures 6 and 7).

Carbonate Chemistry

Because the surface Niskin bottle did not close on a few occasions, surface water was sampled with a bucket. Subsequently these samples were judged to be contaminated. Thus, the following samples were excluded from pH, pCO_2, and aragonite and calcite saturation state figures and tables: 0m on 18 Oct, 1 Nov, and 7 Nov.

The estimated error in pH and pCO_2 was 0.01 and 47µatm, respectively.

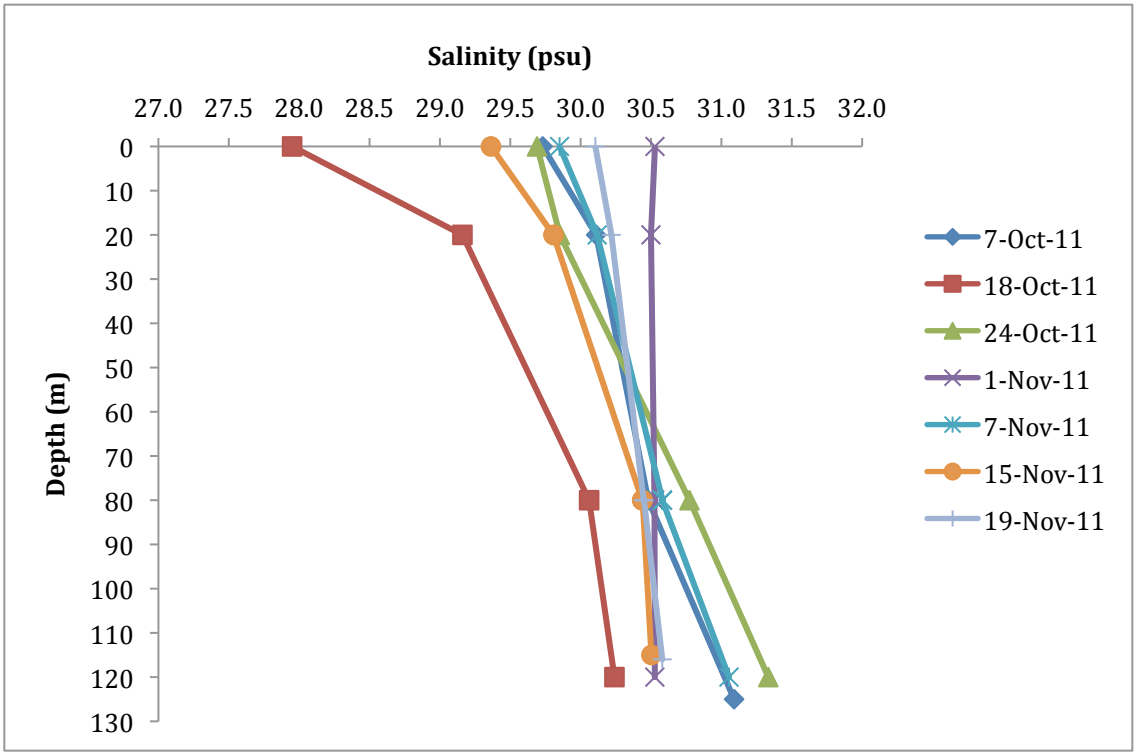

Figure 2: Salinity profiles for North Station.

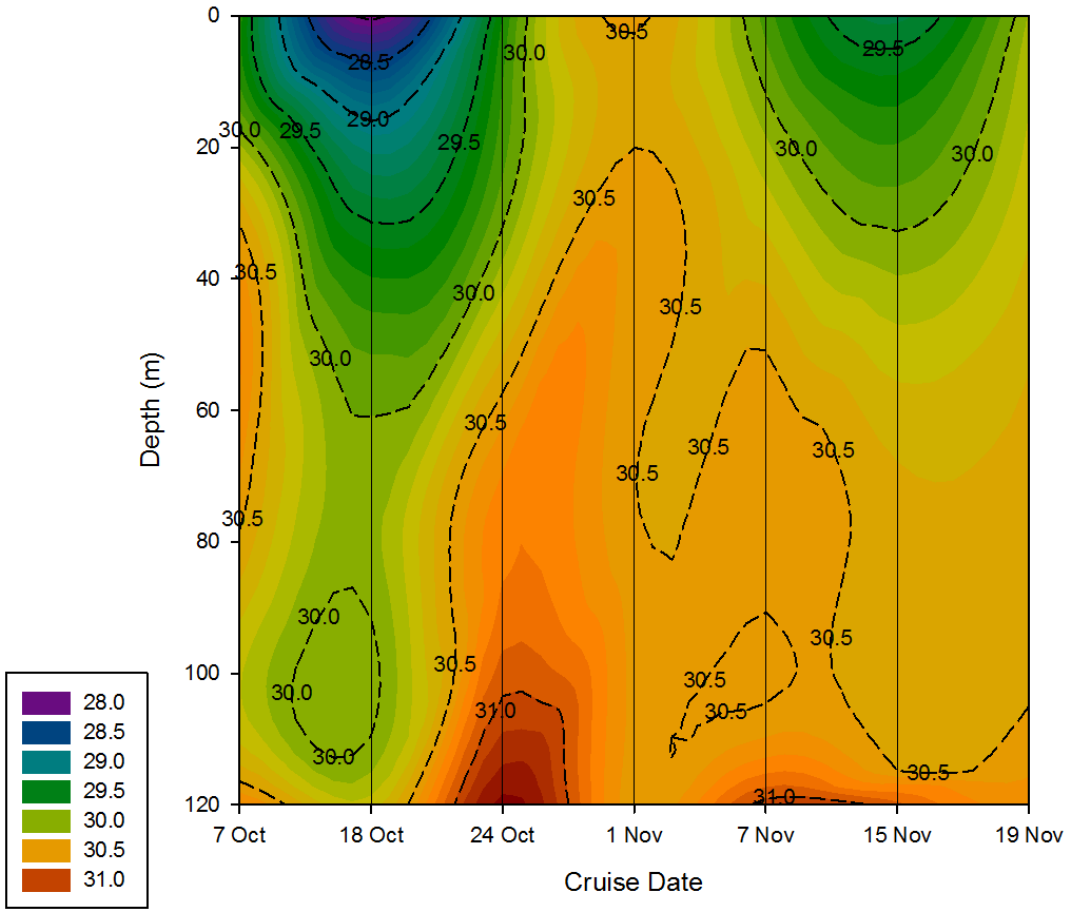

Figure 3: Contour plot of salinity for North Station.

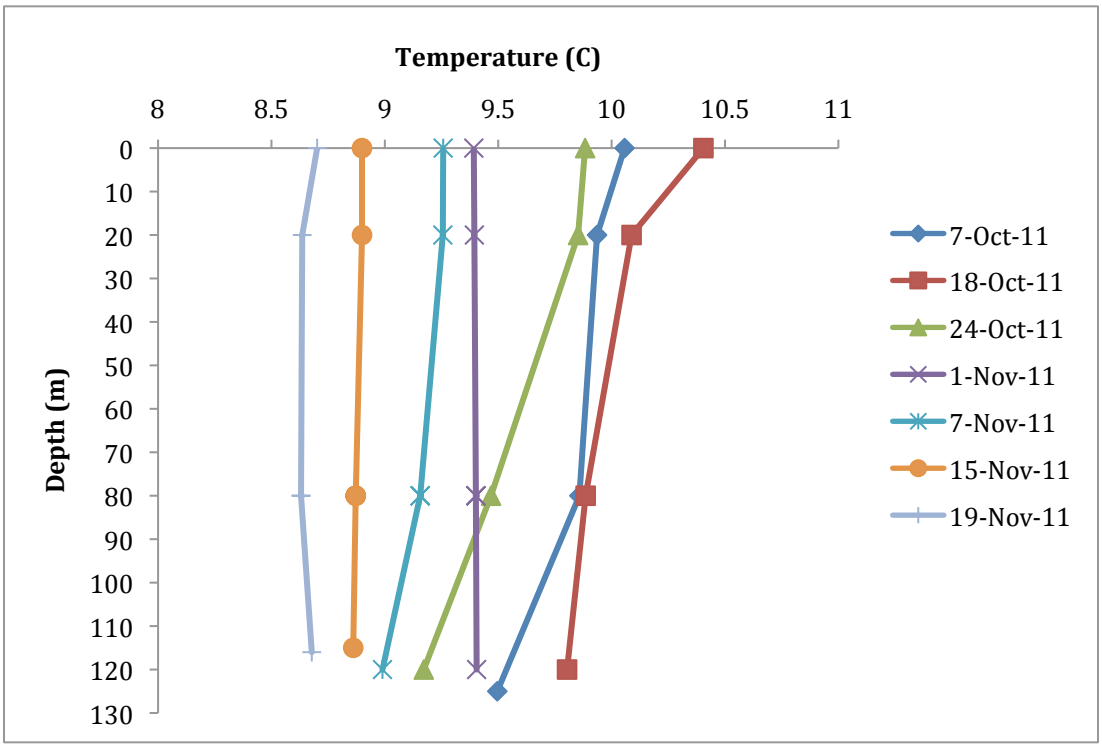

Figure 4: Temperature profiles for North Station.

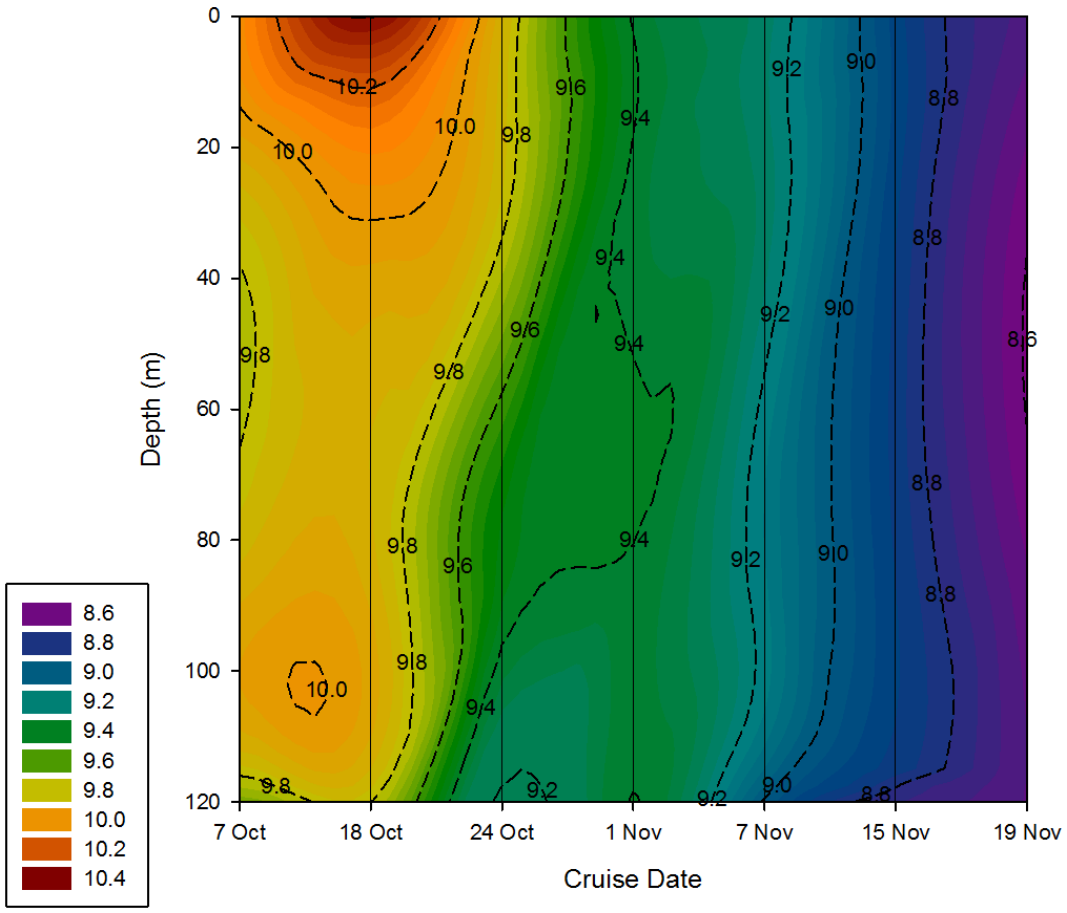

Figure 5: Contour plot of temperature for North Station.

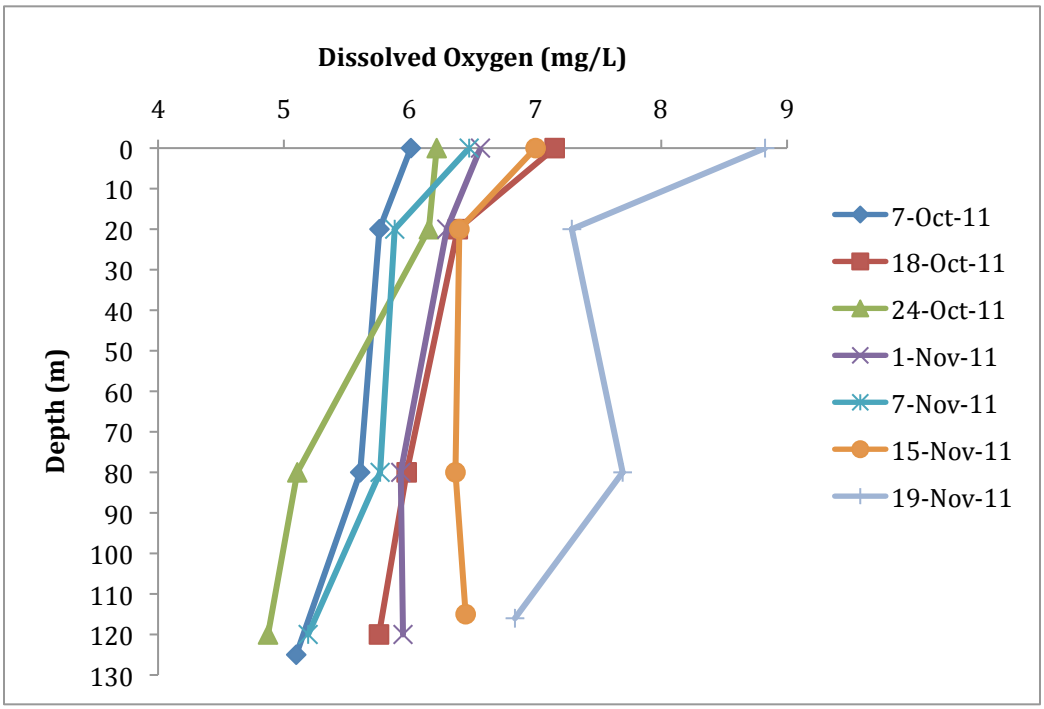

Figure 6: Dissolved oxygen profiles for North Station.

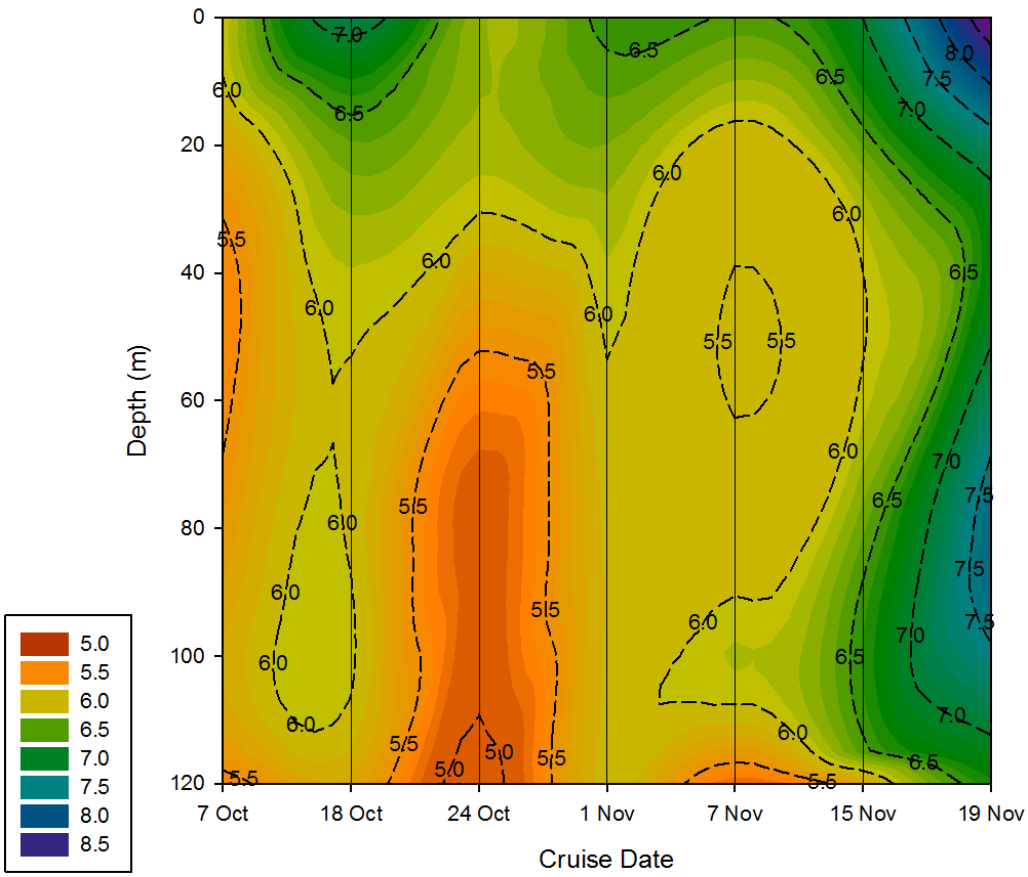

Figure 7: Contour plot of dissolved oxygen for North Station.

During the early part of the time series (7 Oct, 18 Oct, and 24 Oct), the pH decreased with increasing depth (Figures 8 and 9). No trend over time was apparent in surface samples, but pH appeared to decline over time in the deepest samples. The pCO_2 showed similar trends as the pH. The pCO_2 increased with depth on 7 Oct, 18 Oct, and 24 Oct (Figures 10 and 11) and showed little change with depth on 19 Nov. The change over depth was greatest on 1 Nov, 7 Nov, and 15 Nov.

All values of $\Omega_{calcite}$ exceeded 1 (Figures 12 and 13). The highest measured value was at the surface on 7 Oct (Table 3). The lowest values of calcite saturation were observed on at 80m depth on Nov 15 and at all depths on Nov 19.

Aragonite saturation state ($\Omega_{aragonite}$) consistently was less than 1 (Figures 14 and 15). The highest value was observed on 7 Oct at the surface (Table 3). On 7 Oct, 18 Oct, and 24 Oct, values decreased with increasing depth.

Water Mass Sources

Temperature-salinity plots indicated that the primary source of water was a mixture of water from the Strait of Juan de Fuca, the Strait of Georgia, and the surface of the Pacific Ocean (Figure 16). Samples from 7 Oct, 18 Oct, 7 Nov, and 15 Nov showed an influence of a mixture of waters from the Strait of Juan de

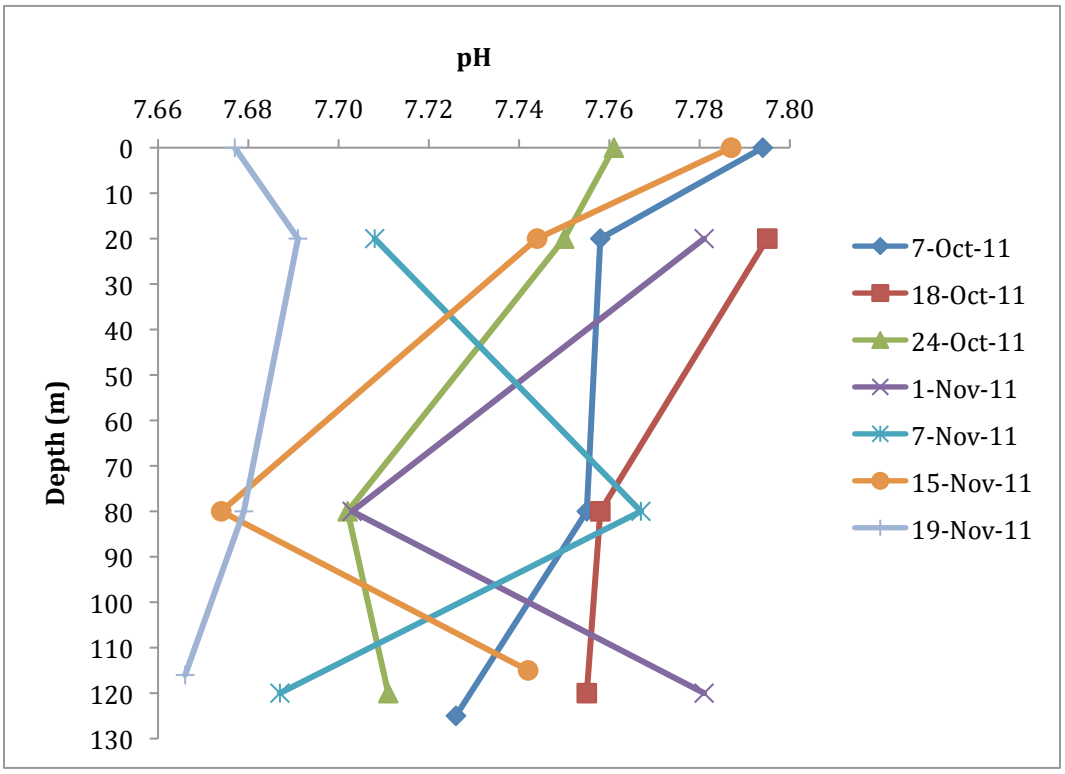

Figure 8: pH profiles for North Station.

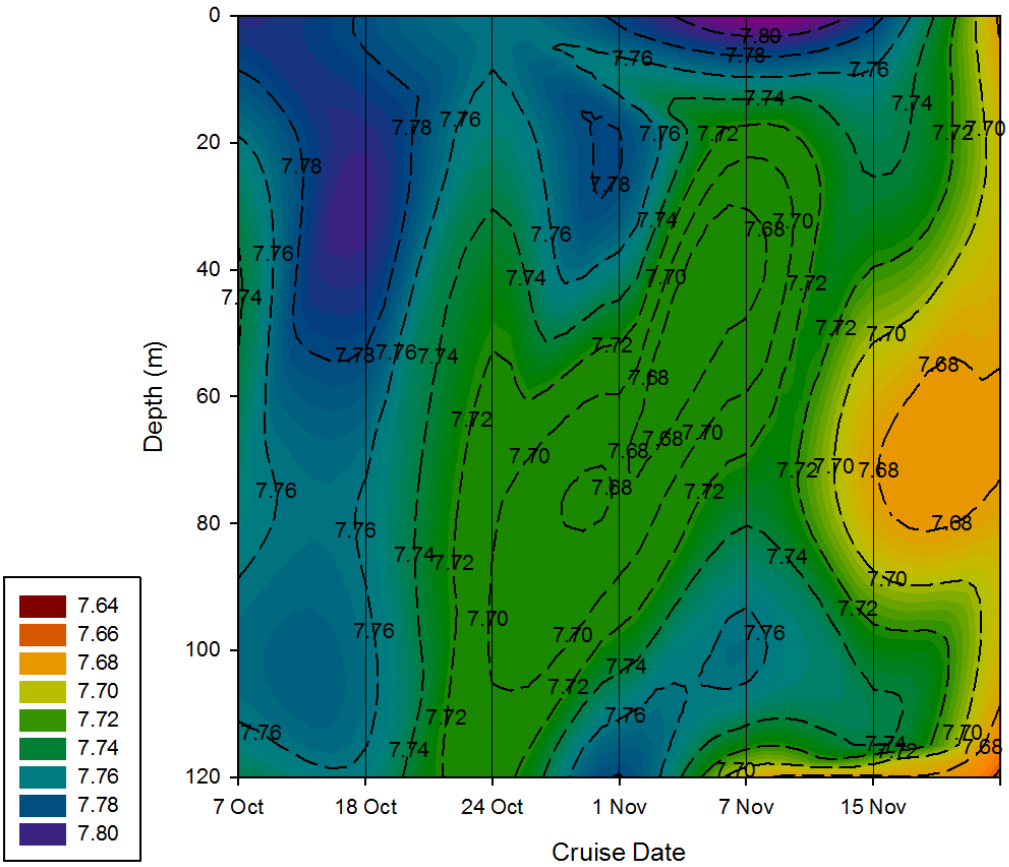

Figure 9: Contour plot of pH for North Station.

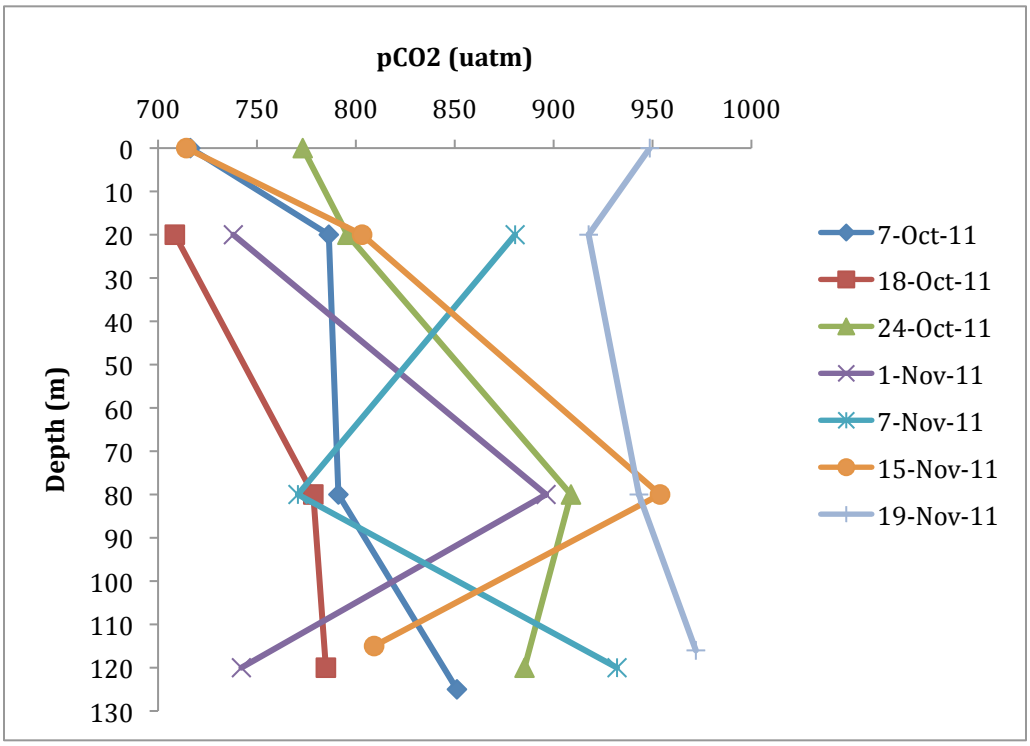

Figure 10: pCO_2 profiles for North Station.

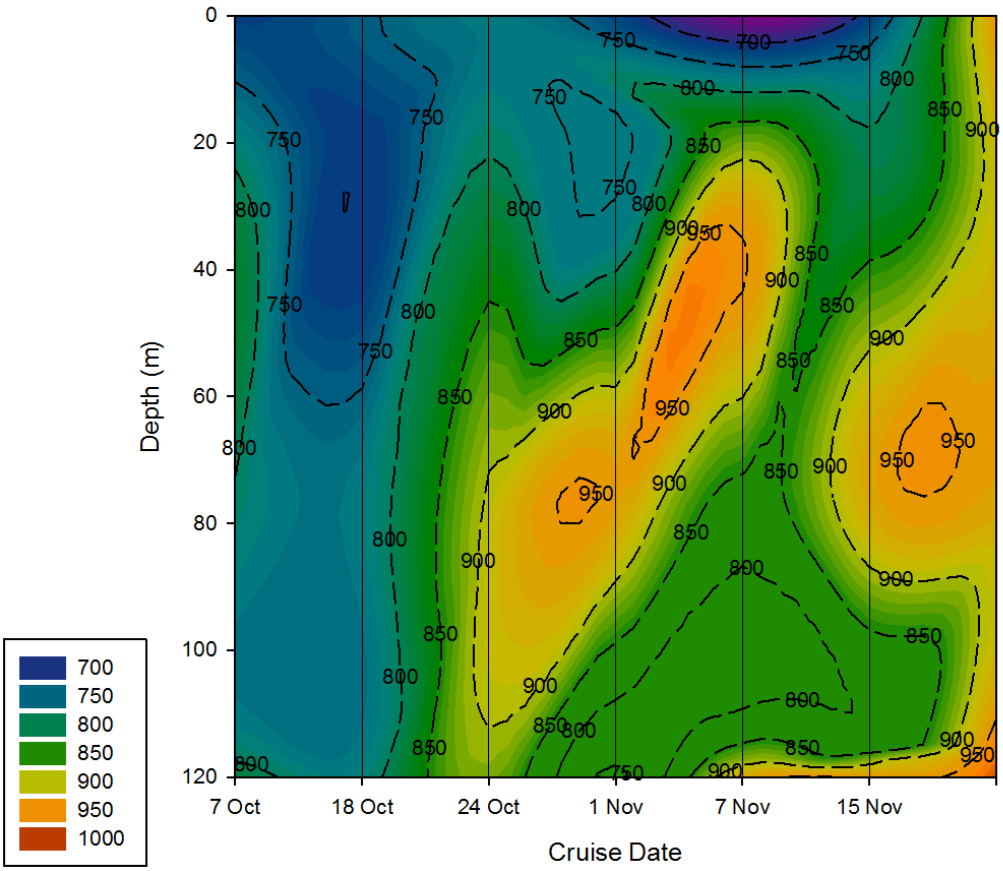

Figure 11: Contour plot of pCO_2 for North Station.

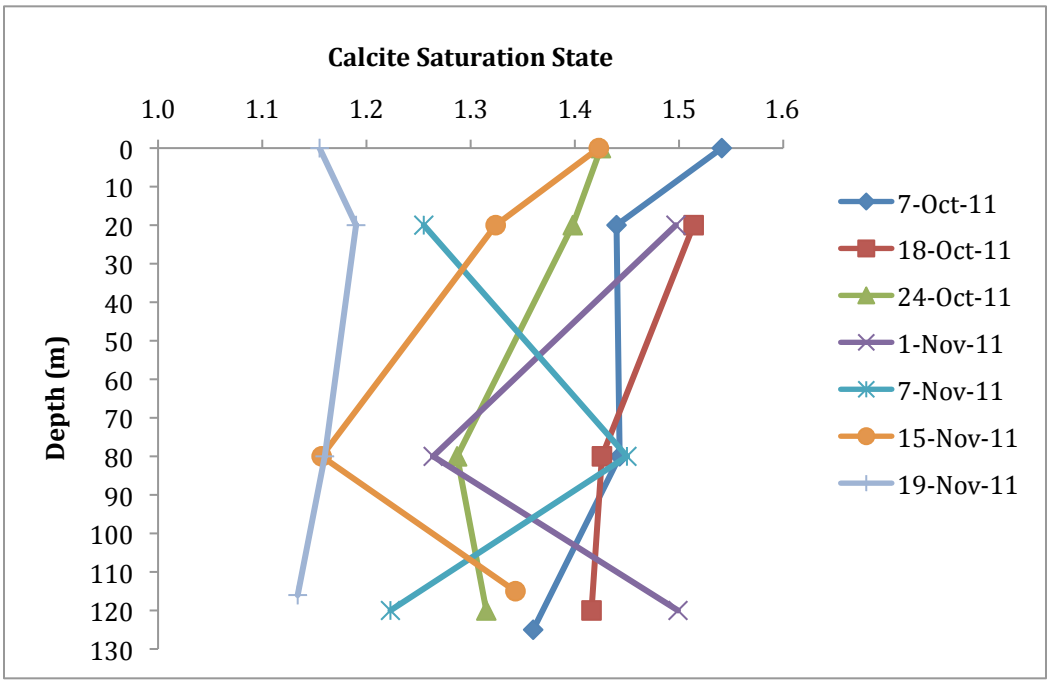

Figure 12: Calcite saturation state profiles for North Station.

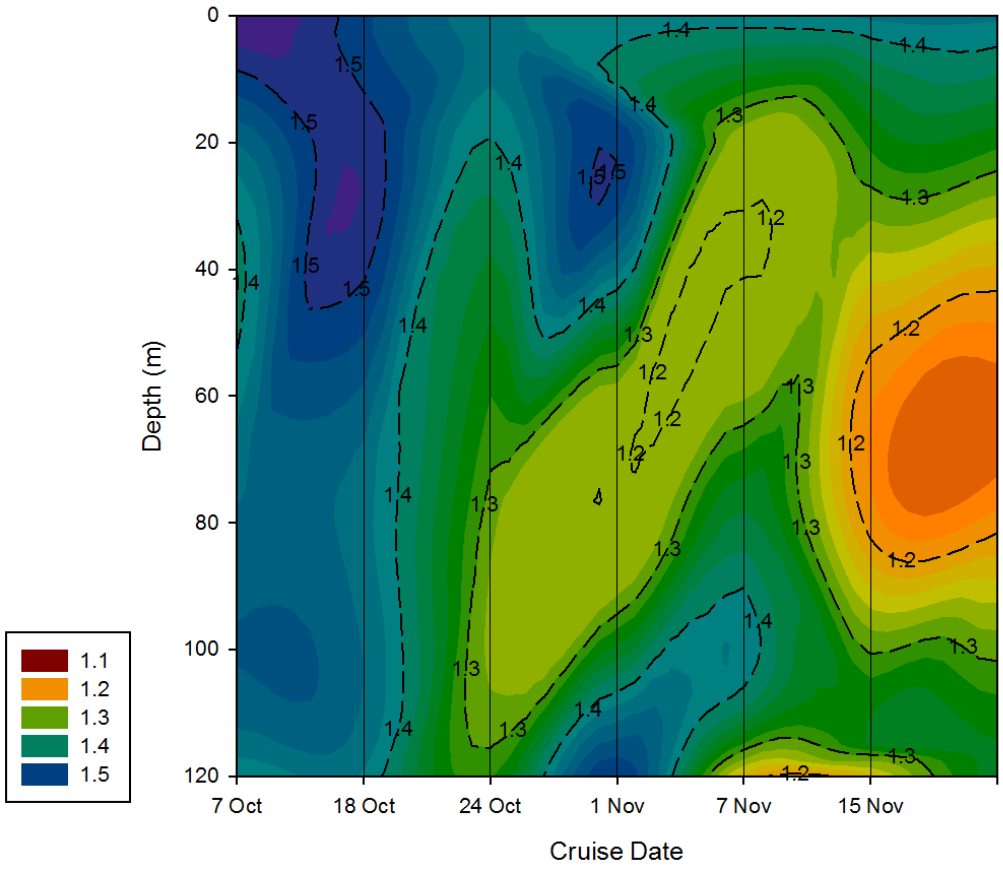

Figure 13: Contour plot of the calcite saturation state for North Station.

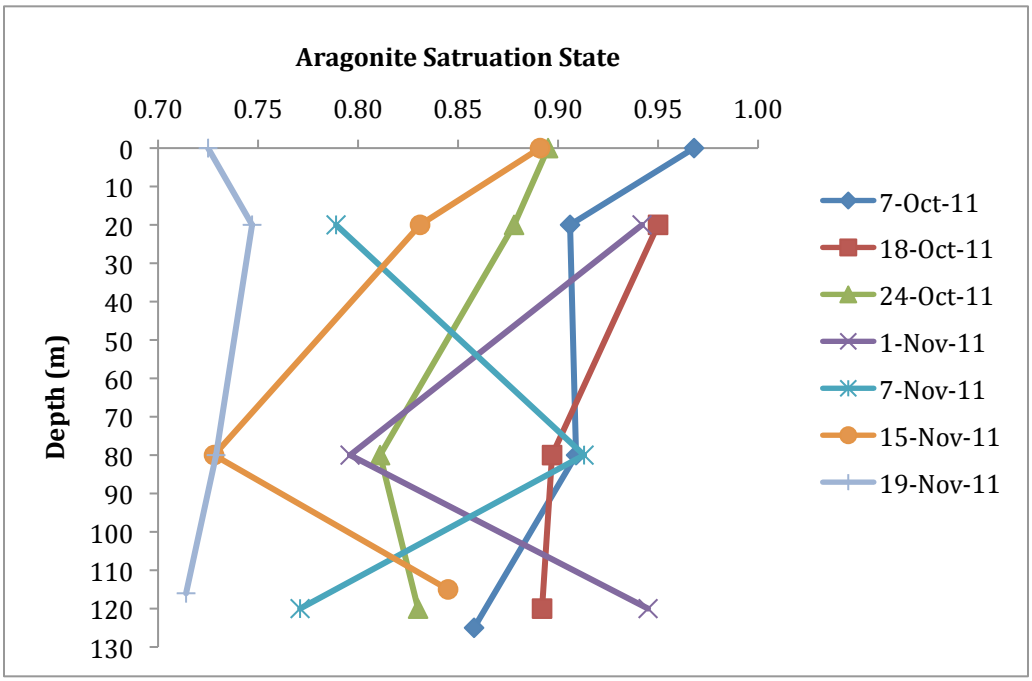

Figure 14: Aragonite saturation state profiles for North Station.

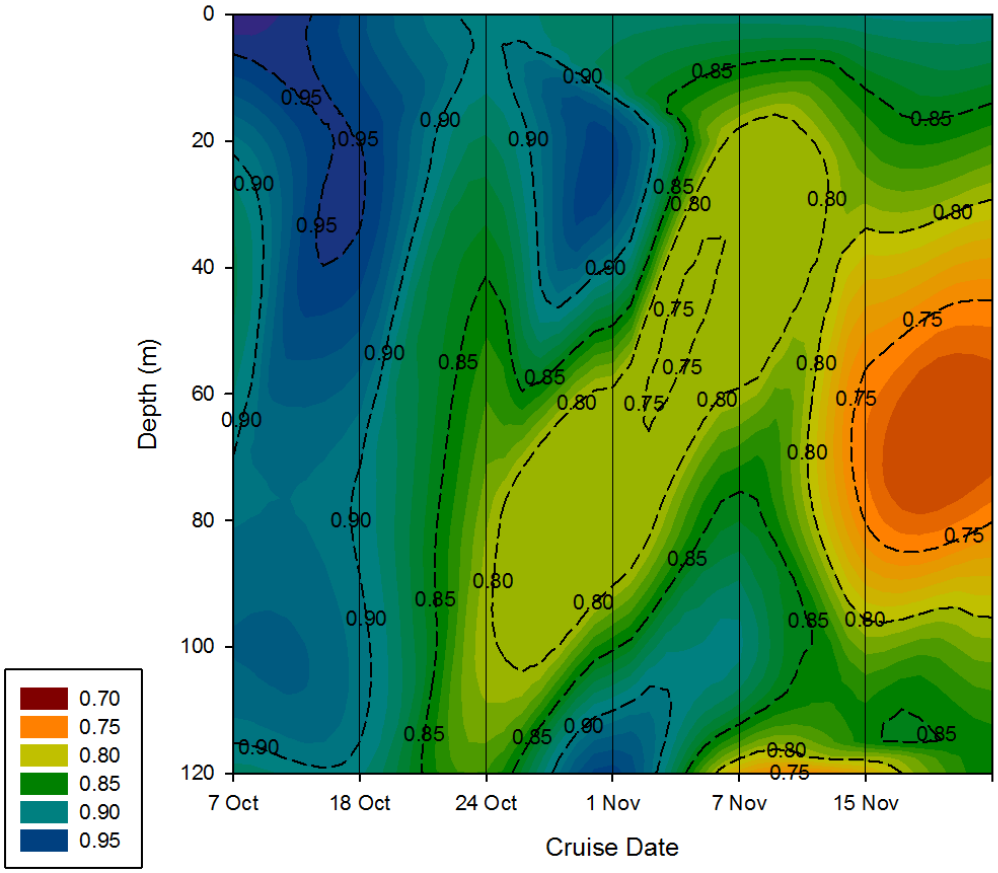

Figure 15: Contour plot of the aragonite saturation state for North Station.

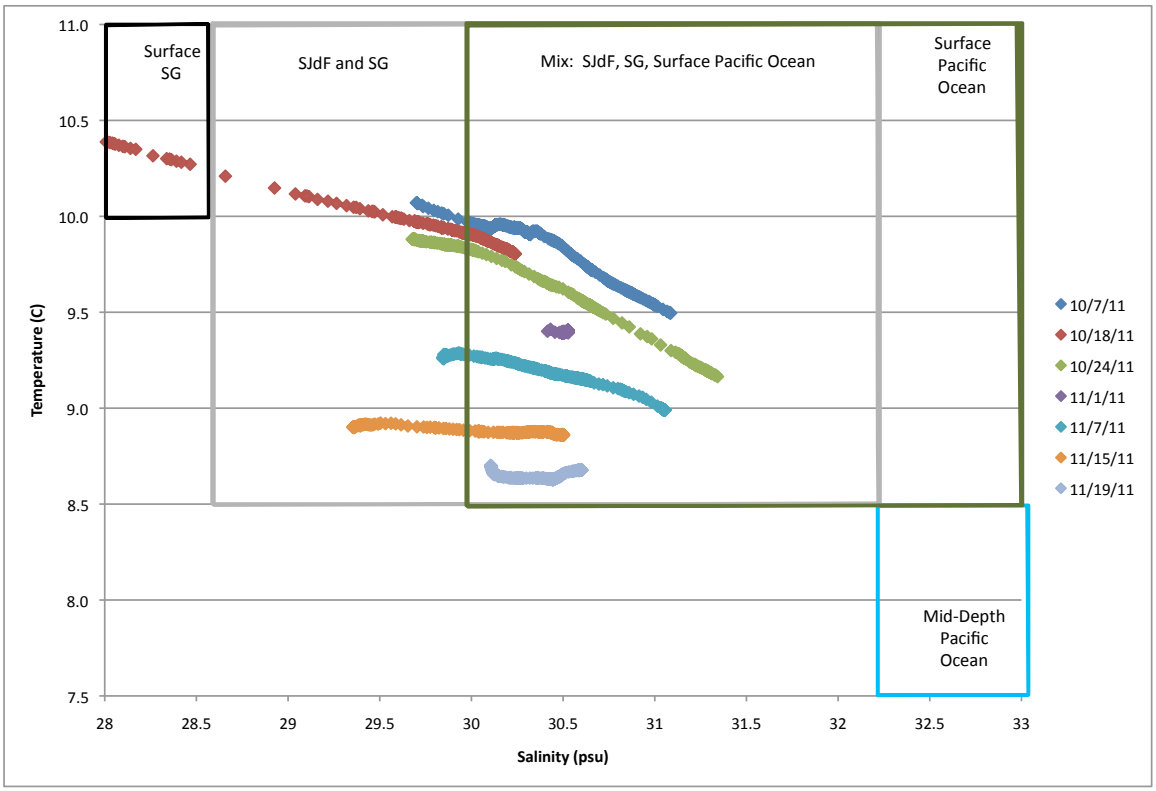

Figure 16: Temperature versus salinity plots for North Station and corresponding sources of water determined from temperature and salinity signatures. SG = Strait of Georgia; SJdF = Strait of Juan de Fuca.

Table 3: Data ranges for pH, pCO_2, calcite and aragonite saturation states, dissolved oxygen, salinity, temperature, and anthropogenic DIC for North Station for the duration of the study.

North Station					
Measurement	**Minimum**	**Maximum**	**Average**	**Standard Deviation**	**Range**
pH	7.67	7.80	7.73	0.04	0.13
pCO_2 (µtam)	708.47	972.37	843.31	84.35	263.93
Calcite	1.13	1.54	1.33	0.13	0.41
Aragonite	0.71	0.97	0.84	0.28	0.25
Dissolved Oxygen (mg/L)	4.87	8.83	6.25	0.84	3.96
Salinity (psu)	27.95	31.33	30.20	0.66	3.38
Temperature (C)	8.63	10.40	9.37	0.50	1.77
Anthropogenic DIC (µmol/kgSW)	11.95	17.35	14.40	1.78	5.40

Fuca and the Strait of Georgia. On 18 Oct, the surface waters were characteristic of surface waters from the Strait of Georgia.

Anthropogenic Input of DIC

The anthropogenic input of DIC was between approximately 12 and 18 µmol/kg SW and there was no trend over depth and time (Tables 3 and 4). On average, pH and the saturation states of calcite and aragonite have declined by 0.03, 0.10, and 0.06, respectively, since the Industrial Revolution (Tables 5, 6, and 7).

South Station

Water Column Properties

The South Station was stratified for the duration of the study with respect to salinity, temperature, and dissolved oxygen (Figures 17 – 22). Temperature and dissolved oxygen decreased with depth, while salinity increased with depth for each time point. Surface temperature decreased throughout the water column over the sampling period, while the pattern at depth was variable. There was no trend over time for salinity and dissolved oxygen over the sampling period. The major pattern over time was an approximately fortnightly variation in the deeper water (>40m) properties between the time points that may be linked to tidal processes.

Table 4. Preindustrial and present DIC (µmol/kgSW) values for North Station.

Depth (m)	7-Oct-11		18-Oct-11		24-Oct-11	
	Pre 1850	2011	Pre 1850	2011	Pre 1850	2011
0	1988	1999			1994	2004
20	2017	2027	1971	1982	2007	2017
80	2038	2048	2014	2024	2076	2085
115						
116						
120			2025	2035	2087	2096
125	2070	2079				

Depth (m)	1-Nov-11		7-Nov-11		15-Nov-11		19-Nov-11	
	Pre 1850	2011	Pre 1850	2011	Pre 1850	2011	Pre 1850	2011
0					1965	1976	2038	2046
20	2013	2024	2025	2033	2007	2016	2040	2048
80	2051	2059	2048	2059	2051	2058	2053	2061
115					2042	2051		
116							2064	2072
120	2042	2053	2078	2086				
125								

Table 5. Preindustrial and present pH values for North Station.

Depth (m)	7-Oct-11		18-Oct-11		24-Oct-11	
	Pre 1850	2011	Pre 1850	2011	Pre 1850	2011
0	7.83	7.79			7.80	7.76
20	7.79	7.76	7.84	7.80	7.79	7.75
80	7.79	7.76	7.79	7.76	7.73	7.70
115						
116						
120			7.79	7.76	7.74	7.71
125	7.76	7.73				

Depth (m)	1-Nov-11		7-Nov-11		15-Nov-11		19-Nov-11	
	Pre 1850	2011	Pre 1850	2011	Pre 1850	2011	Pre 1850	2011
0					7.83	7.79	7.71	7.68
20	7.82	7.78	7.74	7.71	7.78	7.74	7.72	7.69
80	7.73	7.70	7.80	7.77	7.70	7.67	7.71	7.68
115					7.78	7.74		
116							7.70	7.67
120	7.82	7.78	7.72	7.69				
125								

Table 6. Preindustrial and present calcite saturation states for North Station.

Depth (m)	7-Oct-11		18-Oct-11		24-Oct-11	
	Pre 1850	2011	Pre 1850	2011	Pre 1850	2011
0	1.67	1.54			1.54	1.43
20	1.55	1.44	1.65	1.51	1.51	1.40
80	1.56	1.44	1.54	1.43	1.38	1.29
115						
116						
120			1.53	1.42	1.41	1.32
125	1.46	1.36				

Depth (m)	1-Nov-11		7-Nov-11		15-Nov-11		19-Nov-11	
	Pre 1850	2011	Pre 1850	2011	Pre 1850	2011	Pre 1850	2011
0					1.55	1.42	1.23	1.16
20	1.62	1.50	1.34	1.26	1.43	1.32	1.27	1.19
80	1.35	1.26	1.57	1.45	1.23	1.16	1.24	1.16
115					1.45	1.34		
116							1.21	1.13
120	1.62	1.50	1.31	1.22				
125								

Table 7. Preindustrial and present aragonite saturation states for North Station.

Depth (m)	7-Oct-11		18-Oct-11		24-Oct-11	
	Pre 1850	2011	Pre 1850	2011	Pre 1850	2011
0	1.05	0.97			0.97	0.90
20	0.98	0.91	1.03	0.95	0.95	0.88
80	0.98	0.91	0.97	0.90	0.87	0.81
115						
116						
120			0.96	0.89	0.89	0.83
125	0.92	0.86				

Depth (m)	1-Nov-11		7-Nov-11		15-Nov-11		19-Nov-11	
	Pre 1850	2011	Pre 1850	2011	Pre 1850	2011	Pre 1850	2011
0					0.97	0.89	0.77	0.73
20	1.02	0.94	0.82	0.77	0.90	0.83	0.80	0.75
80	0.85	0.80	0.82	0.77	0.78	0.73	0.78	0.73
115					0.91	0.85		
116							0.76	0.71
120	1.02	0.95	0.82	0.77				
125								

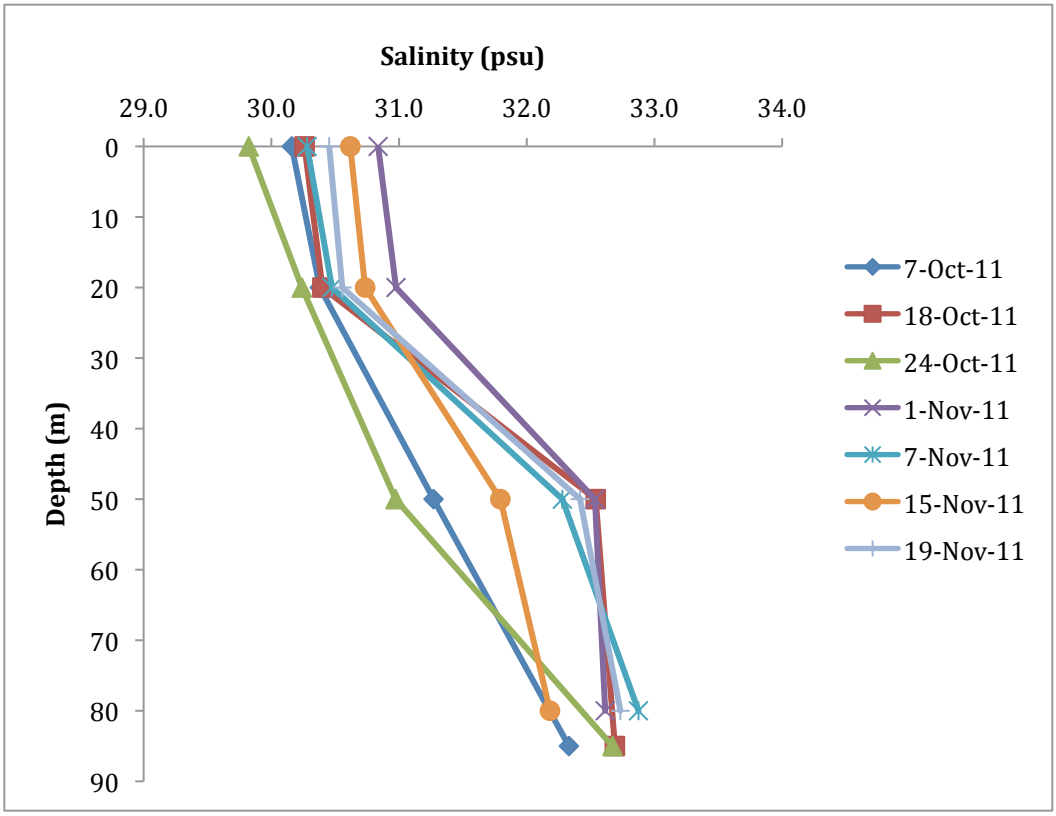

Figure 17: Salinity profiles for South Station.

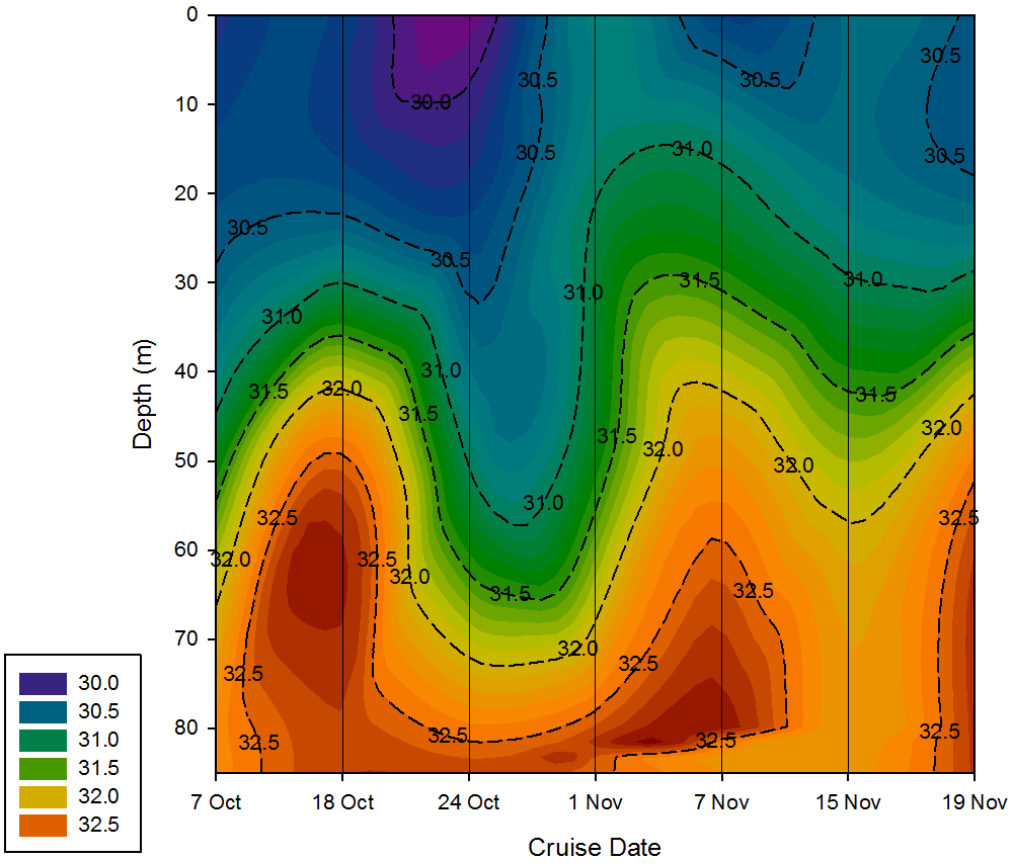

Figure 18: Contour plot of salinity for South Station.

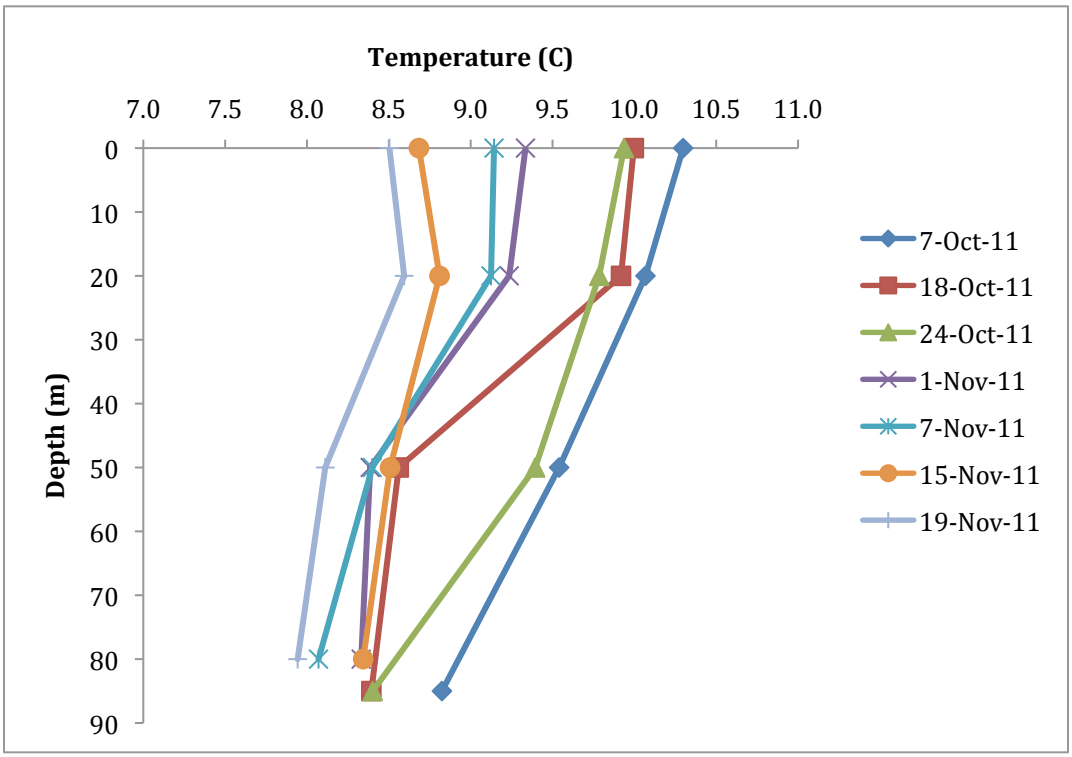

Figure 19: Temperature profiles for South Station.

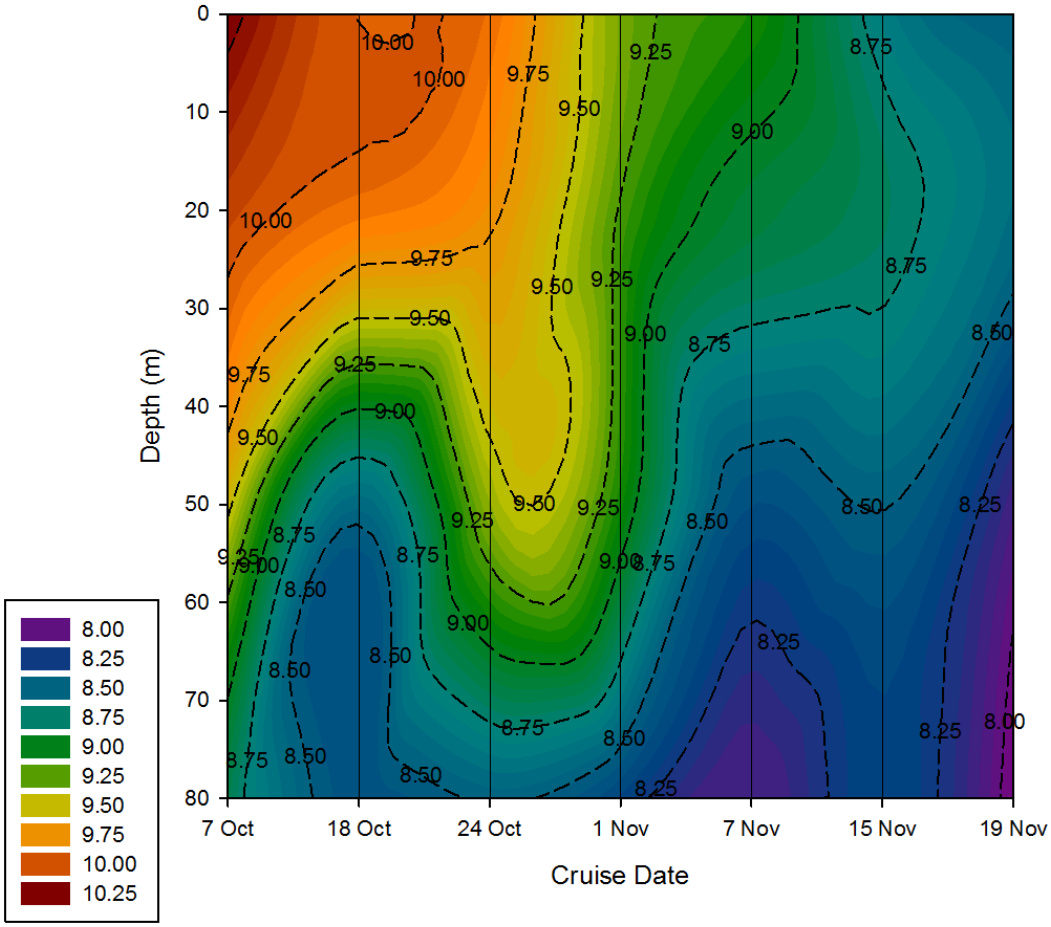

Figure 20: Contour plot of temperature for South Station.

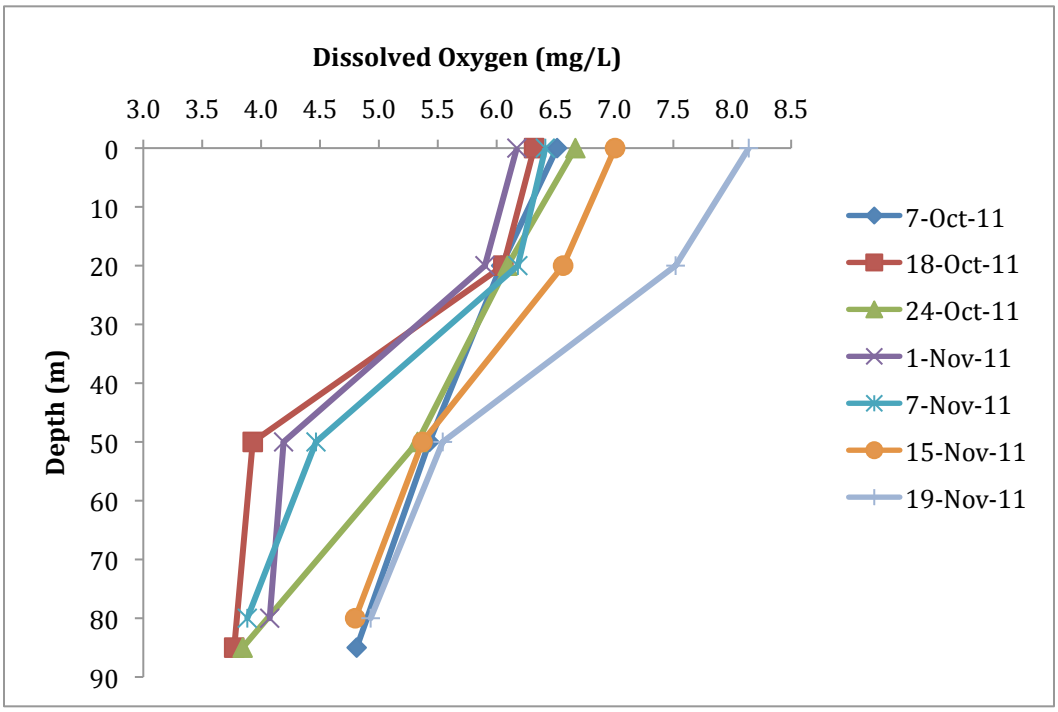

Figure 21: Dissolved oxygen profiles for South Station.

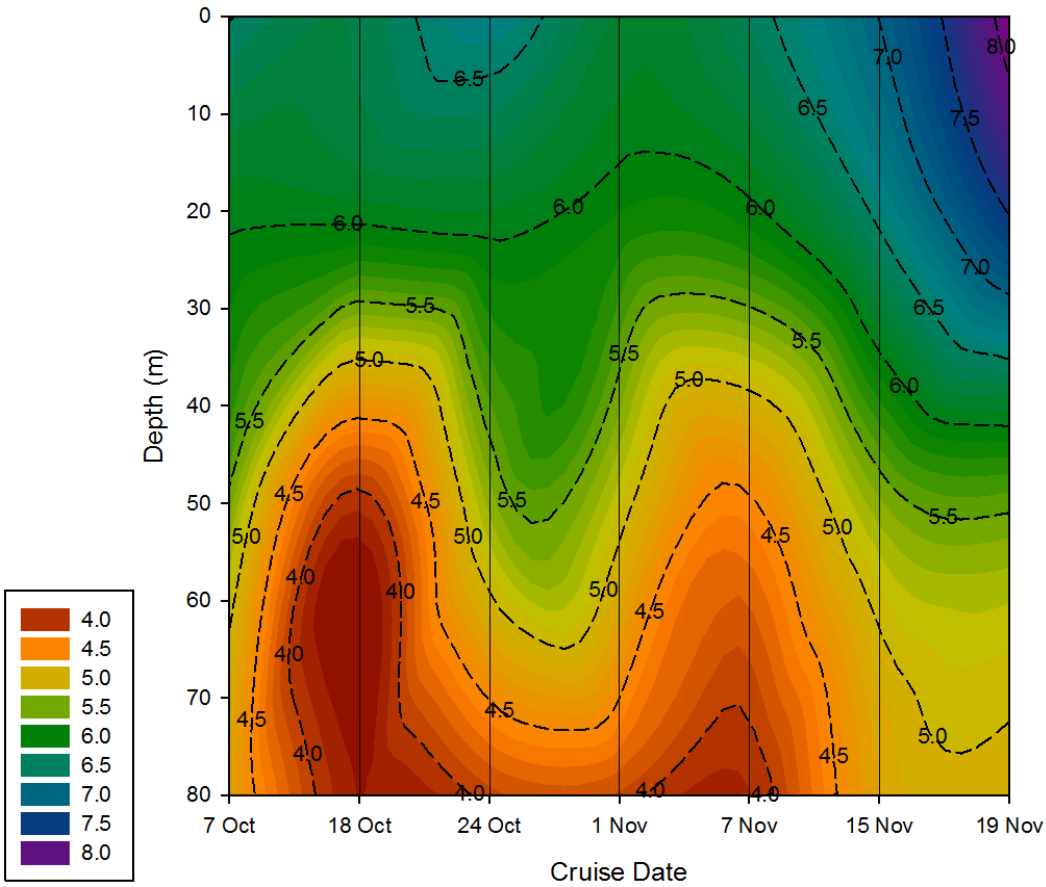

Figure 22: Contour plot of dissolved oxygen for South Station.

Carbonate Chemistry

The following points were excluded from pH, pCO_2, and calcite and aragonite saturation state figures and tables: 1 November at 50m and 7 November at 20m. The analytical results for carbonate variables were in conflict with the water column properties; thus, the data for those points are considered invalid. The surface sample on 18 Oct was also excluded from figures and tables due to sample contamination as described in the North Carbonate Chemistry section.

The estimated error in pH and pCO_2 was 0.01 and 47µatm, respectively.

A difference was observed between the first three sampling time points (7 Oct, 18 Oct, and 24 Oct) and the final four time points (1 Nov, 7 Nov, 15 Nov, and 19 Nov) (Figures 23 and 24) in that the earlier pH measurements were higher than the later ones. Overall, pH declined over the sampling time period at all depths.

The pCO_2 measurements also showed a similar pattern. The pCO_2 for the earlier three time points was lower than the later four measurements (Figures 25 and 26). Variation was smallest at the surface and greatest at the deepest measurements.

Calcite saturation state ($\Omega_{calcite}$) was consistently above 1 (Table 8; Figures 27 and 28). Values decreased over time at the surface, 20m, and the deepest depth measured. The greatest variation over time occurred at 50m for each time point,

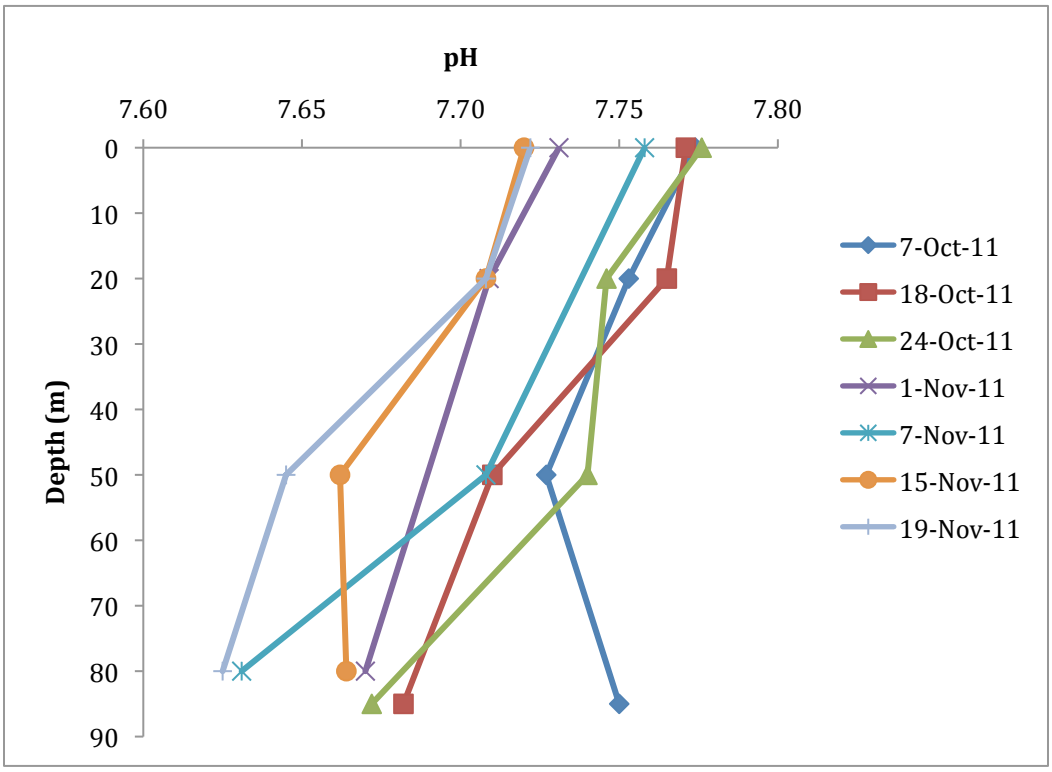

Figure 23: pH profiles for South Station.

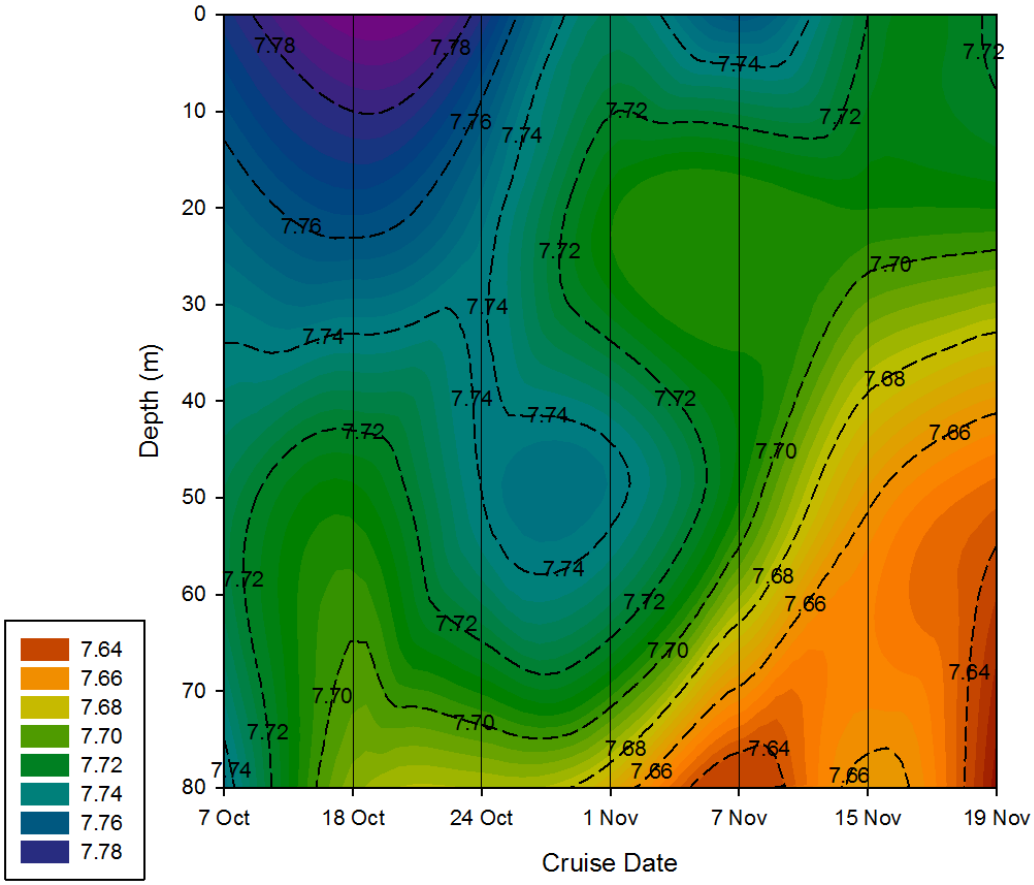

Figure 24: Contour plot of pH for South Station.

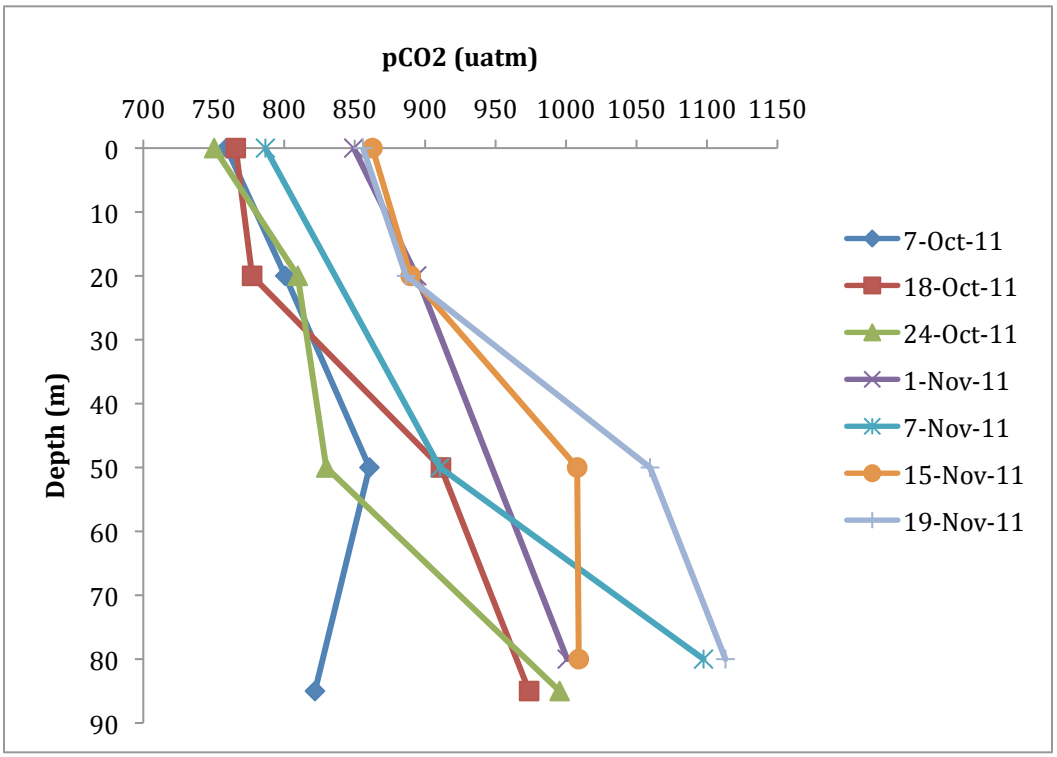

Figure 25: pCO_2 profiles for South Station.

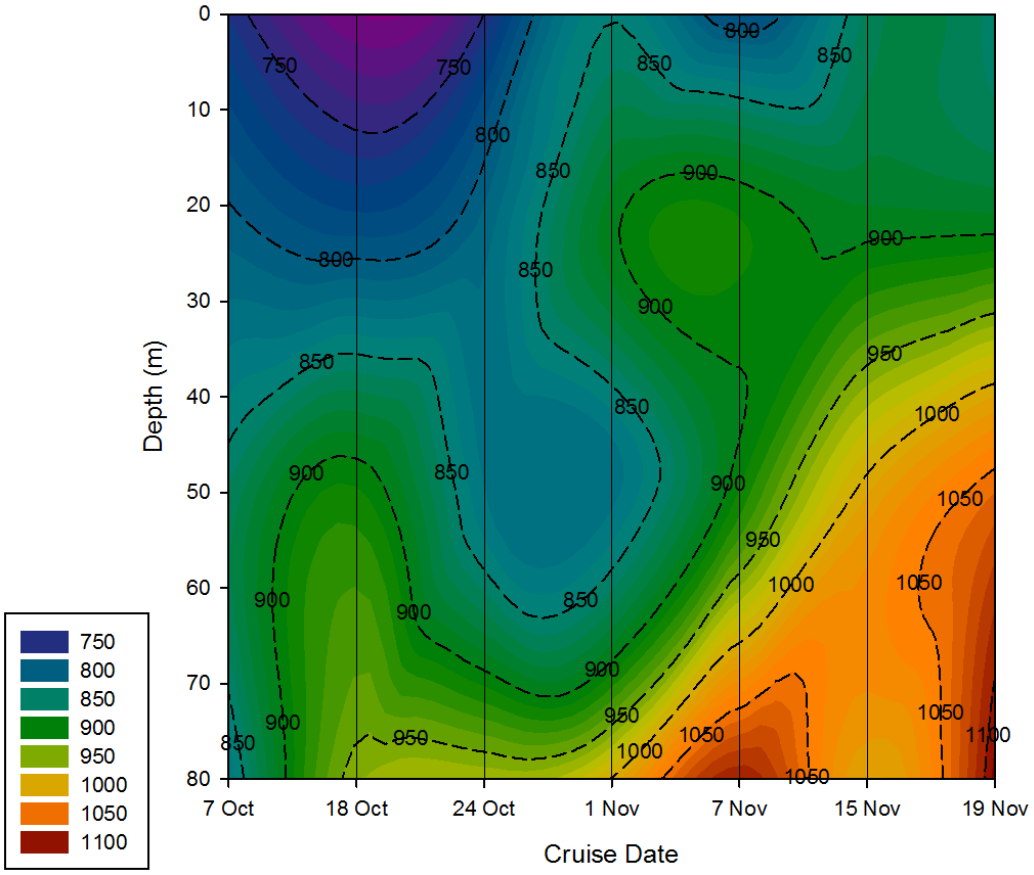

Figure 26: Contour plot of pCO_2 for South Station.

Table 8: Data ranges for pH, pCO_2, calcite and aragonite saturation states, dissolved oxygen, salinity, temperature, and anthropogenic DIC for South Station for the duration of the study.

South Station					
Measurement	**Minimum**	**Maximum**	**Average**	**Standard Deviation**	**Range**
pH	7.63	7.78	7.71	0.04	0.15
pCO_2 (µatm)	750.28	1113.14	900.51	105.17	362.86
Calcite	1.10	1.52	1.32	0.12	0.42
Aragonite	0.70	0.96	0.83	0.07	0.26
Dissolved Oxygen (mg/L)	3.77	8.14	5.60	1.18	4.37
Salinity (psu)	29.82	32.87	31.35	1.03	3.05
Temperature (C)	7.94	10.30	8.97	0.71	2.35
Anthropogenic DIC (µmol/kgSW)	10.94	16.40	13.76	1.62	5.46

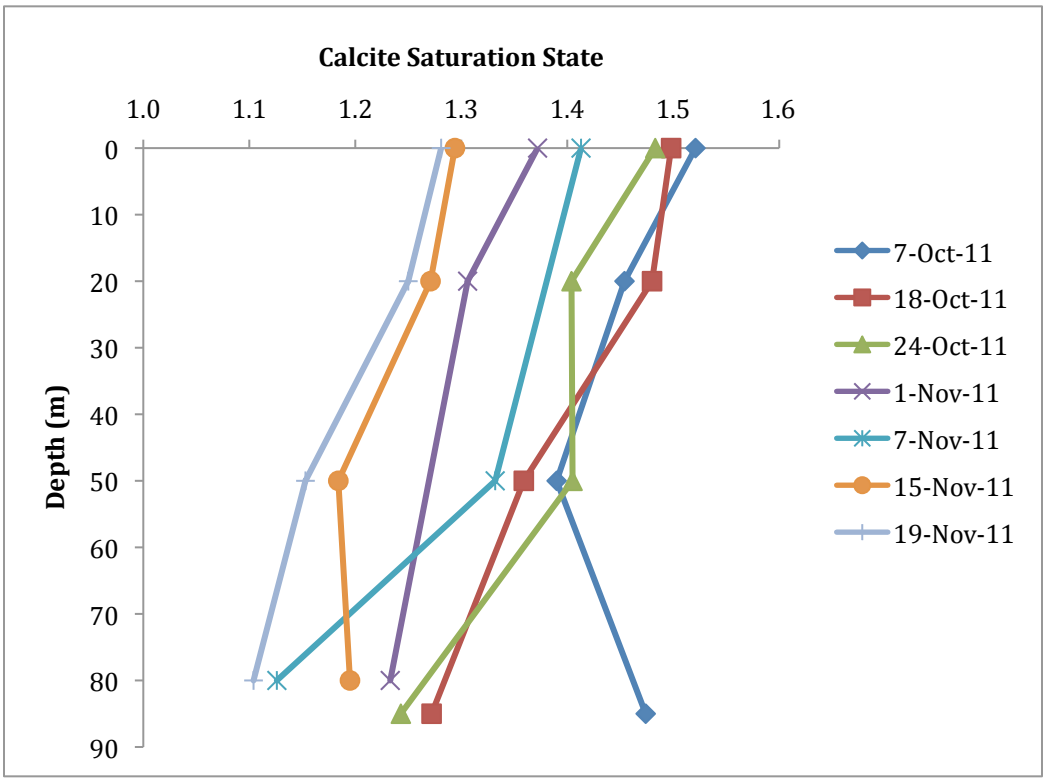

Figure 27: Calcite saturation state profiles for South Station.

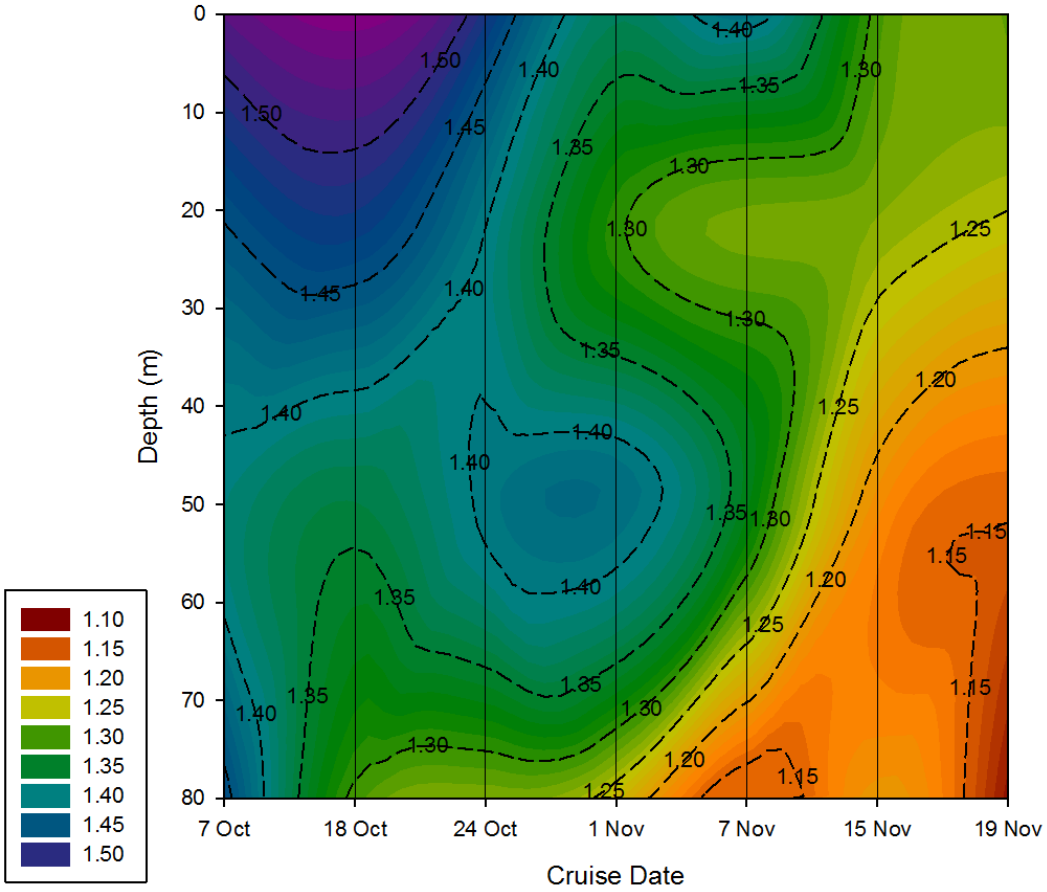

Figure 28: Contour plot of the calcite saturation state for South Station.

which was consistent with the other water properties as well (T, S, DO).

Aragonite saturation state ($\Omega_{aragonite}$) consistently was less than 1 (Figures 29 and 30). The initial three measurements were distinctly higher than the final four, and had a smaller range of values (Table 8). There was an overall trend for decreasing saturation state over time at surface, 20m, and 80m measurements.

Water Mass Sources

Temperature-salinity plots indicated that the primary source of water at the South Station was a combination of the Strait of Juan de Fuca, the Strait of Georgia, and surface water from the Pacific Ocean (Figure 31). There was no influence from the surface waters of the Strait of Georgia. At deeper depths on 7 Oct, 18 Oct, 24 Oct, and 1 Nov, there was an influence from the surface waters of the Pacific Ocean. At the deepest depths sampled on 18 Oct, 24 Oct, 1 Nov, 7 Nov, 15 Nov, and 19 Nov, the water's temperature-salinity signature corresponded to mid-depths in the Pacific Ocean.

Anthropogenic Input of DIC

The anthropogenic input of DIC was between approximately 11 - 16 µmol/kg SW and there was a general decline over the sample period (Tables 8 and 9). On average, pH and the saturation states of calcite and aragonite have declined by 0.03, 0.09, and 0.06, respectively, since the Industrial Revolution (Tables 10, 11, and 12).

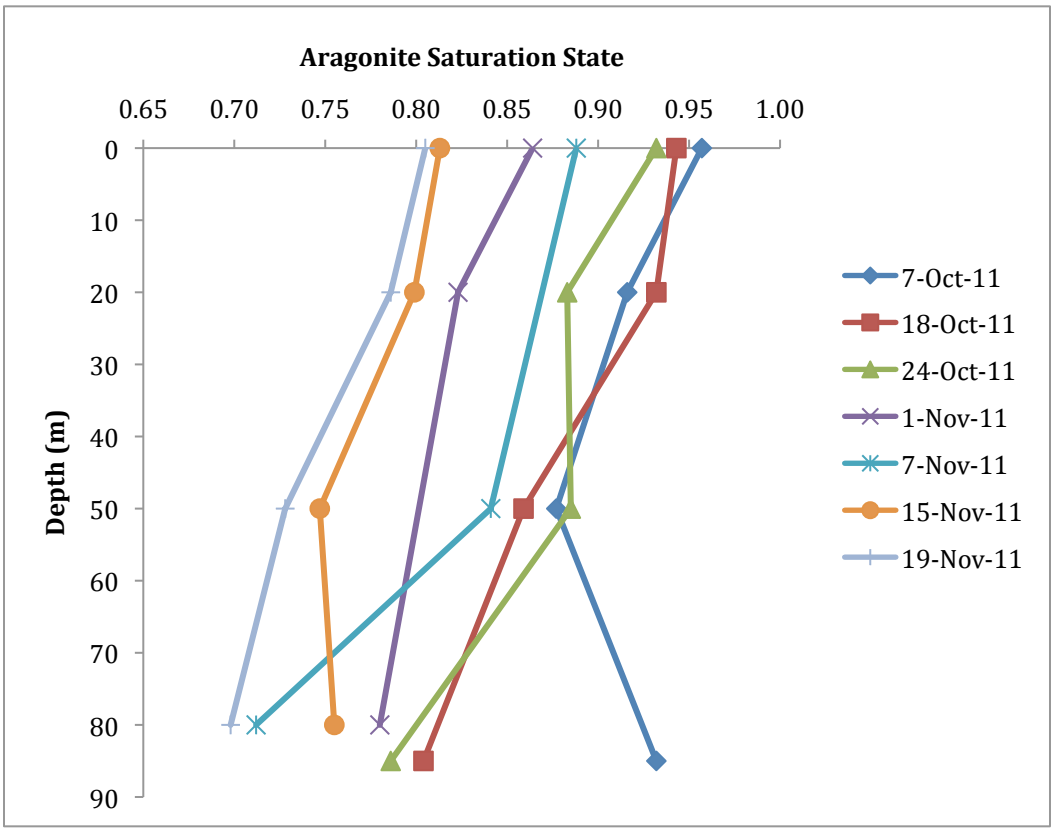

Figure 29: Aragonite saturation state profiles for South Station.

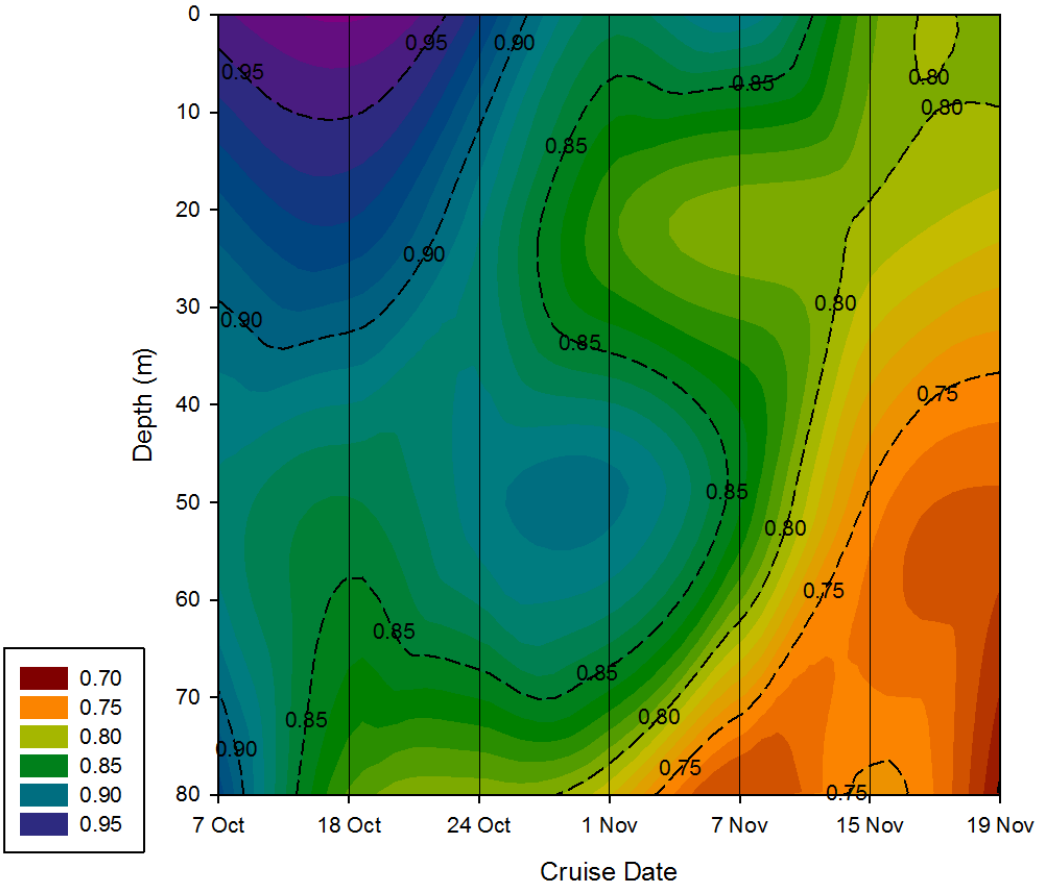

Figure 30: Contour plot of the aragonite saturation state for South Station.

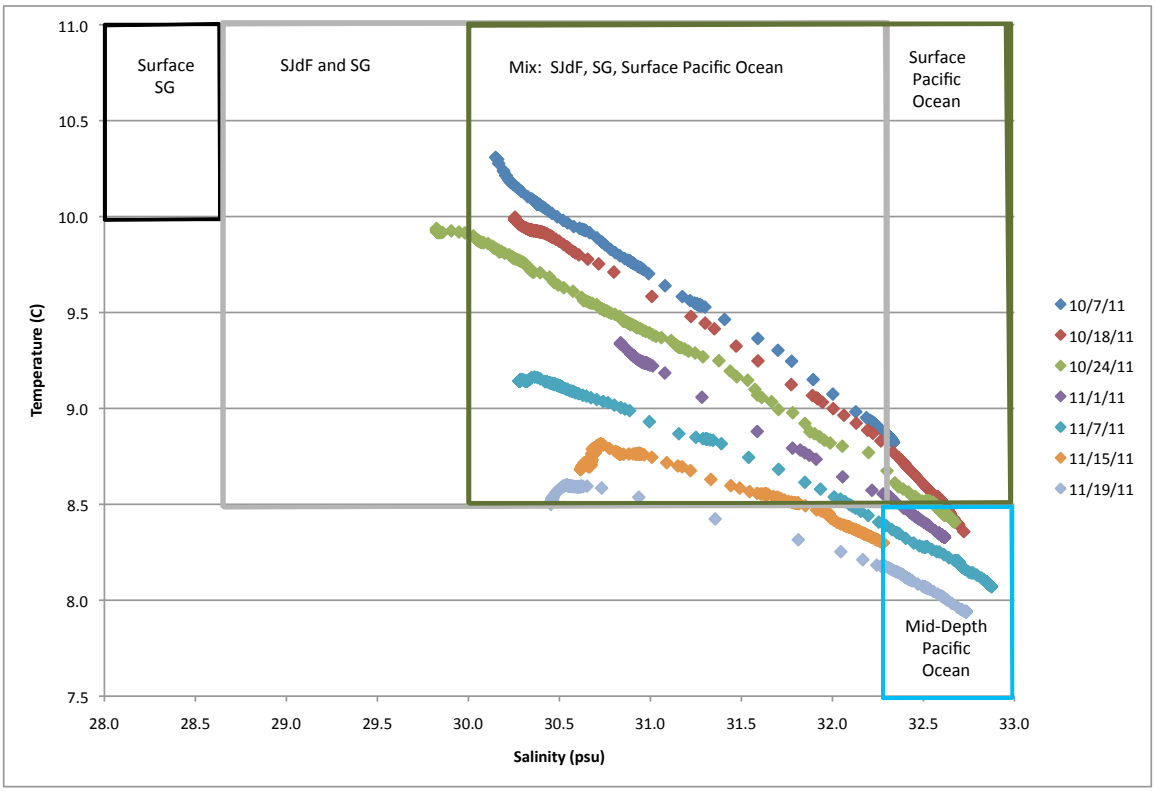

Figure 31: Temperature versus salinity plots for South Station and corresponding sources of water determined from temperature and salinity signatures. SG = Strait of Georgia; SJdF = Strait of Juan de Fuca.

Table 9. Preindustrial and present DIC (µmol/kgSW) values for South Station.

Depth (m)	7-Oct-11		18-Oct-11		24-Oct-11	
	Pre 1850	2011	Pre 1850	2011	Pre 1850	2011
0	2016	2026			2001	2011
20	2036	2046	2030	2041	2026	2036
50	2082	2091	2147	2156	2067	2076
85	2123	2133	2162	2170	2161	2169

Depth (m)	1-Nov-11		7-Nov-11		15-Nov-11		19-Nov-11	
	Pre 1850	2011	Pre 1850	2011	Pre 1850	2011	Pre 1850	2011
0	2060	2069	2029	2039	2050	2058	2043	2052
20	2069	2078			2060	2068	2052	2061
50			2137	2146	2122	2130	2158	2165
80	2162	2170	2173	2181	2143	2151	2176	2183

Table 10. Preindustrial and present pH values for South Station.

Depth (m)	7-Oct-11		18-Oct-11		24-Oct-11	
	Pre 1850	2011	Pre 1850	2011	Pre 1850	2011
0	7.81	7.77			7.81	7.78
20	7.79	7.75	7.80	7.77	7.78	7.75
50	7.76	7.73	7.74	7.71	7.77	7.74
85	7.78	7.75	7.71	7.68	7.70	7.67

Depth (m)	1-Nov-11		7-Nov-11		15-Nov-11		19-Nov-11	
	Pre 1850	2011	Pre 1850	2011	Pre 1850	2011	Pre 1850	2011
0	7.76	7.73	7.79	7.76	7.75	7.72	7.76	7.72
20	7.74	7.71			7.74	7.71	7.74	7.71
50			7.74	7.71	7.69	7.66	7.67	7.65
80	7.70	7.67	7.66	7.63	7.69	7.66	7.65	7.63

Table 11. Preindustrial and present calcite saturation states for South Station.

Depth (m)	7-Oct-11		18-Oct-11		24-Oct-11	
	Pre 1850	2011	Pre 1850	2011	Pre 1850	2011
0	1.64	1.52			1.61	1.48
20	1.57	1.45	1.60	1.48	1.51	1.40
50	1.49	1.39	1.45	1.36	1.51	1.41
85	1.59	1.47	1.35	1.27	1.32	1.24

Depth (m)	1-Nov-11		7-Nov-11		15-Nov-11		19-Nov-11	
	Pre 1850	2011	Pre 1850	2011	Pre 1850	2011	Pre 1850	2011
0	1.47	1.37	1.53	1.41	1.39	1.29	1.38	1.28
20	1.40	1.31			1.36	1.27	1.34	1.25
50			1.42	1.33	1.26	1.18	1.22	1.15
80	1.31	1.23	1.19	1.13	1.27	1.20	1.17	1.10

Table 12. Preindustrial and present aragonite saturation states for South Station.

Depth (m)	7-Oct-11		18-Oct-11		24-Oct-11	
	Pre 1850	2011	Pre 1850	2011	Pre 1850	2011
0	1.04	0.96			1.01	0.93
20	0.99	0.92	1.01	0.93	0.95	0.88
50	0.94	0.88	0.92	0.86	0.95	0.89
85	1.00	0.93	0.86	0.80	0.84	0.79

Depth (m)	1-Nov-11		7-Nov-11		15-Nov-11		19-Nov-11	
	Pre 1850	2011	Pre 1850	2011	Pre 1850	2011	Pre 1850	2011
0	0.93	0.86	0.96	0.89	0.87	0.81	0.86	0.81
20	0.88	0.82			0.86	0.80	0.84	0.79
50			0.90	0.84	0.79	0.75	0.77	0.73
80	0.83	0.78	0.75	0.71	0.80	0.76	0.74	0.70

Fall Transition

The regime shift in the fall typically occurs in mid-October; however, the atmospheric 2011 fall transition occurred approximately on 15 September (Figure 32). Although the samples were collected during conditions that were overall characterized by downwelling, there were pulses of upwelling on the outer coast of Washington during that time, as measured from La Push (Figure 33). The South Station receives coastal influences due to its location in the Strait of Juan de Fuca. Upwelling events occurred between 27 Sept – 1 Oct; 12 – 16 Oct; 22 – 27 Oct; 30 Oct – 2 Nov; and 10 – 11 Nov (Figure 33). Deep water upwelled from the outer coast has a markedly different signal than that which normally circulates through the Strait of Juan de Fuca side in upwelling times. Upwelled waters are denser, colder, more saline, and less oxygenated (Davenne and Masson 2001). There is evidence of water with these characteristics moving through the South Station on 1 Nov and 7 Nov (Figures 16 – 22). Samples taken on these days exhibited influences from the mid-Pacific Ocean and surface Pacific Ocean (Figure 31), indicating a possible link between upwelling events and the associated carbonate chemistry.

Fraser River Plume

The discharge of the Fraser River has been noted as having influences on the water column at the North Station (Pers. Comm., Jan Newton). Strong pulses of river water discharge are represented in salinity data at this site by freshening at

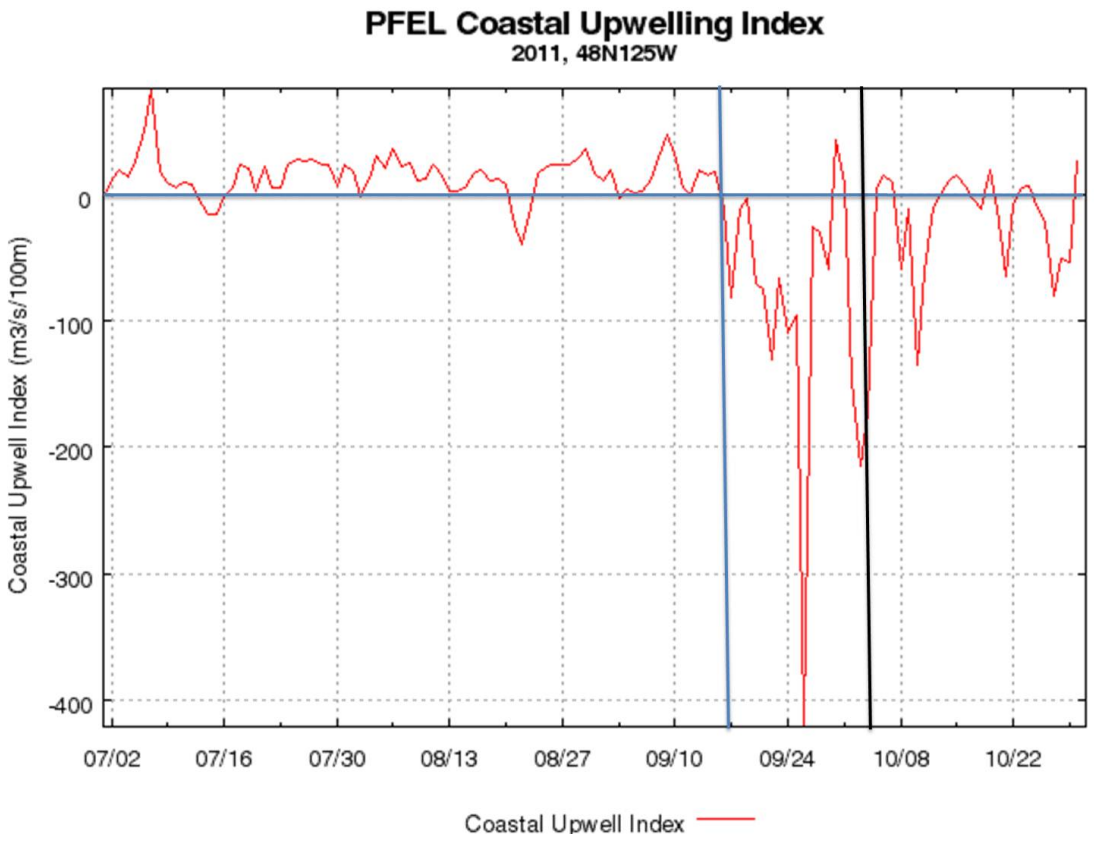

Figure 32: The fall transition from summer upwelling to winter downwelling, as measured from La Push, Washington between 1 July and 1 November 2011 as measured by the Pacific Fisheries Environmental Laboratory (PFEL). The horizontal blue line indicates the transition line: above this line indicates upwelling and below the line indicates downwelling. The vertical blue line shows where the transition was and the vertical black line shows the start of the sampling period.

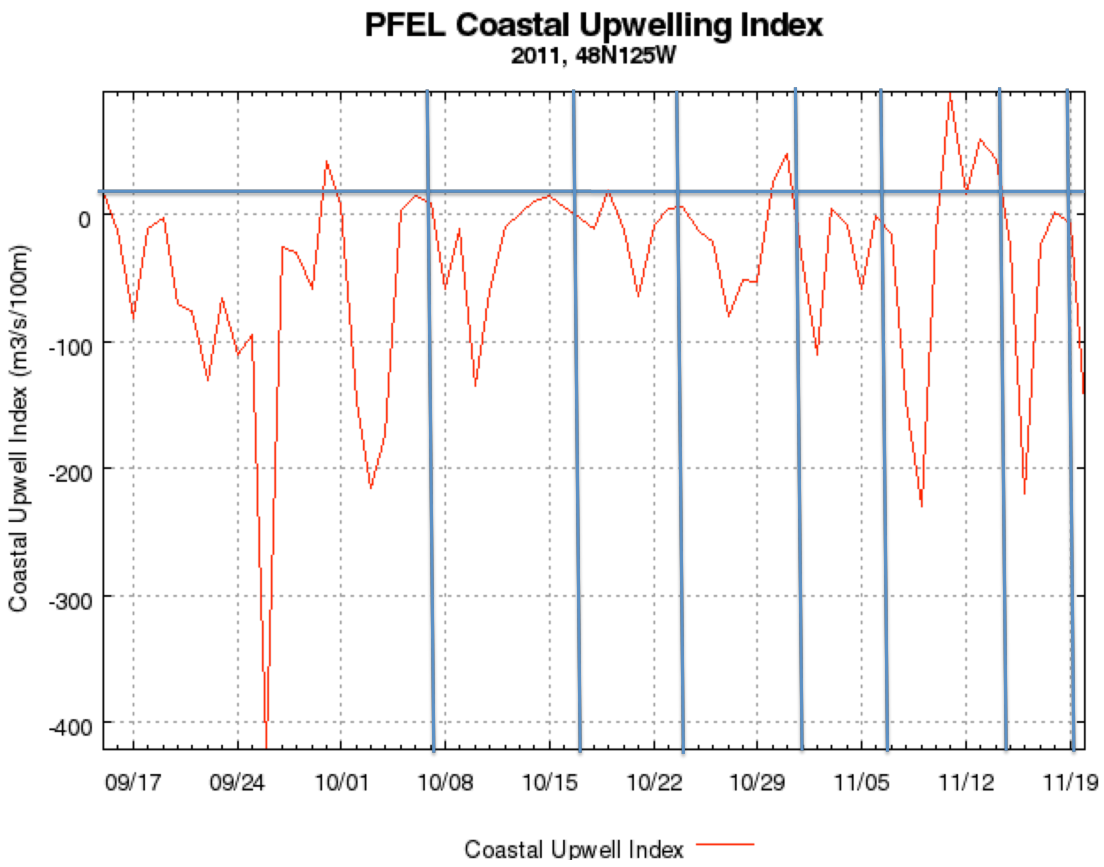

Figure 33: Upwelling events during the sampling period as measured from La Push, Washington as measured by the Pacific Fisheries Environmental Laboratory (PFEL). Data above the horizontal line indicate upwelling, whereas data below the horizontal line indicate downwelling. Vertical lines indicate days in which the water column was sampled for this study.

the surface layer. Rivers have been reported to be lower in pH than coastal waters (Salisbury et al. 2008). On 18 Oct, there was a decline in pH from the surface to 20m (Figures 8 and 9), which could indicate the intrusion of fresher surface water from the Fraser River. This decline in pH corresponds with changes in other variables, for example, an increase in pCO_2 and a decrease in calcite and aragonite saturation states.

Freshwater inputs were strongest on 18 Oct and 15 Nov. Given the increase in discharge from the Fraser River as measured by Environment Canada at Hope (BC, Canada) (Environment Canada 2012) between approximately 27 Sept and 5 Oct, and from approximately 14 Oct to 18 Oct, it is possible that the Fraser River was the source of the decrease in surface salinity in samples collected on 18 Oct (Figure 34). There was no strong pulse prior to the fresher surface water on 15 Nov.

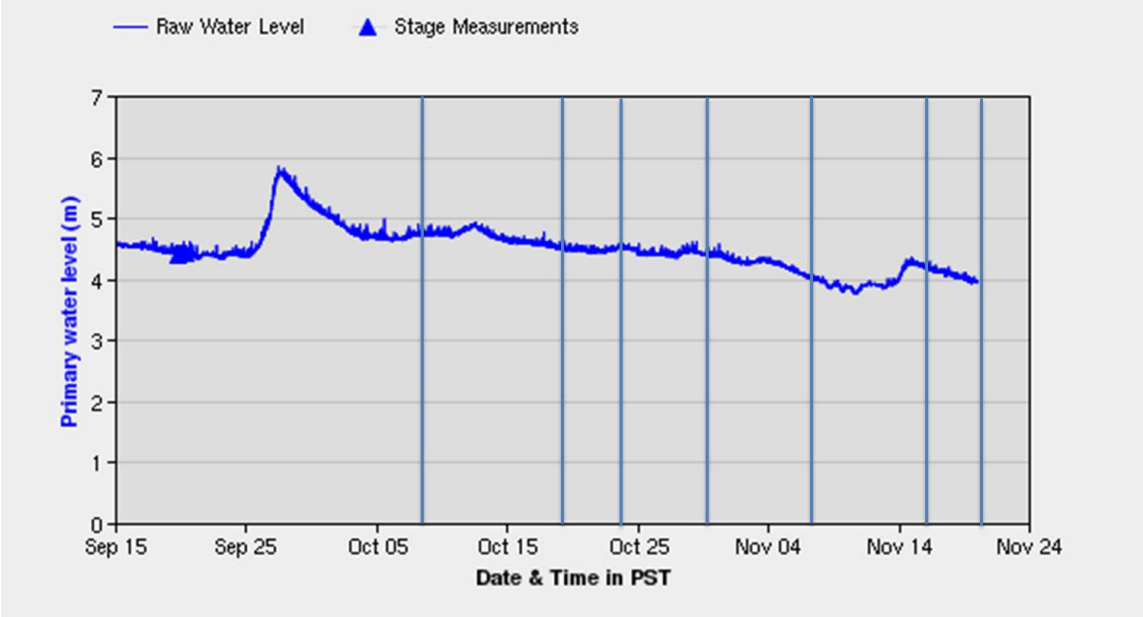

Figure 34: Fraser River discharge from 15 Sept to 20 Nov 2011 as measured from Hope, BC (Canada). The vertical blue lines show the days that the water column was sampled for this study.

Discussion

This study was the first of its kind in this region with respect to location and relatively small scales. It demonstrates high levels of variation over relatively small spatial and short temporal scales in all carbonate chemistry variables examined. The results are vital to understanding the impacts of the contributions of ocean acidification to this region and corresponding effects to organisms.

The pH values in this study are similar those measured in the neighboring region of Puget Sound (Feely et al. 2010). The variation observed in this study (0.15) was smaller than that of 0.5 reported by Feely et al. (2010). The range of values in these two studies does, however, overlap. The variation observed in this study could be less because the sample locations were closer to each other and were taken during one season, whereas the measurements by Feely et al. (2010) were taken from a larger area around Puget Sound over the course of two seasons.

The predicted rate of decline in pH is -0.0017pH/year, which is less than the natural variability observed in many locations (Hofmann et al. 2011). This holds true for the ranges in this study (0.13 – 0.15 at the North and South stations, respectively); however the variation observed in this study is much lower than the range for pH variation reported by Hofmann et al. (2011) in eastern Pacific Estuarine/ Near shore sites (0.499 – 0.992, respectively). The mean pH values at the South and North Stations observed in this study were lower than the mean

pH values in Hofmann et al. (2011) for the Pacific Estuarine/ Near shore sites; however, the minimum value was higher in the current study (7.54) than the minimum value in Hofmann et al. (2011) (7.435). In this study, the highest value was 7.80, which was lower than the highest value of 8.427 found in Hofmann et al. (2011) for the eastern Pacific sites.

Through NANOOS, the UW and NOAA operate a buoy off the coast of La Push, Washington (47.97^{O}N, 124.95^{O}W), as part of NOAA's Ocean Acidification Program and the US Integrated Ocean Observing System (IOOS). The buoy measures the levels of CO_2 in the surface layer of the ocean and in the air. The measurements were not taken continuously throughout this study's sampling period; however, there were measurements performed until 13 October 2011 when the buoy was retrieved for maintenance. The mean measurement of fCO_2 from this buoy from 7 Oct (the first day of sampling during the current study) to 13 Oct was 346 (±10) µatm. The mean measurement of fCO_2 during the current study was 882 (±124) µatm. The range of variation observed in samples taken at the North and South Stations was greater than the range of variation observed at the La Push buoy, with no overlap in measurements made at La Push versus the North and South Stations. This observation could indicate that factors other than upwelling of corrosive water on the outer coast influence seawater carbonate chemistry in the San Juan Archipelago.

As CO_2 is added to the ocean, the dissociation of calcium carbonate occurs. The saturation states of calcite and aragonite are lower in colder high-latitude waters due to the temperature-driven increase in $CaCO_3$ solubility (Feely et al. 2004). Measurements of calcium carbonate saturation state are critical to an understanding of changes in buffering capacity and organismal response to ocean acidification.

The solubility of calcite is 50% higher than that of aragonite (Logan 2010). Calcite saturation states exceeded 1 at the North Station for all values except one. At the South Station, all values exceeded 1. These results indicate that overall, this region is saturated with respect to calcite; however, these values may not be indicative of deposition in this region because some organisms require saturation states of 4 to 6 deposition to occur (Feely et al. 2009). In this study, no measurements of the saturation state of aragonite exceeded 1, indicating that conditions were unfavorable for deposition of aragonite. Similar to calcite, however, many organisms require a saturation state to be from 2 to 4 for deposition of aragonite (Feely et al. 2009).

The contribution of anthropogenic DIC to seawater at the North and South stations (10.94µatm to 17.35µatm) was lower than that of the open ocean (50µatm to 60µatm) (Sabine et al. 2002). Feely et al. (2010) reported similar results in Puget Sound. Because high Revelle factors indicate a low anthropogenic CO_2 signal, these results are attributable to the higher Revelle

factors in coastal areas. The Revelle factors in this study varied from 16.9 to 18.9, whereas the typical value in the open ocean is 10. Coastal systems have lower pH as compared to the open ocean, and are thus less capable of taking up CO_2 from the atmosphere.

The North Station was well mixed, so one can infer that the mixing of the atmospheric fCO_2 was equivalent across all depths. The South Station remained stratified for the duration of the study, so it can be assumed that the surface values are close approximations to the anthropogenic input; however, the values at depth are most likely overestimated. There was a fair amount of input from the mid depths of the Pacific Ocean to the South Station; as a result, the anthropogenic fraction of DIC is an overestimate, as the anthropogenic signature resulting from CO_2 addition is smaller at this station.

The spatial and temporal variation in carbonate chemistry observed in this study indicates the need for measurements to be taken at fine spatial and temporal scales. There are limited studies on variation on relatively short temporal scales (e.g., Hofmann et al. 2011), and hence limited understanding of the variation experienced by organisms. The pH and carbonate saturation states observed in this study were consistently lower than those of the surface of the open ocean, and are already lower than values predicted for the open ocean at the end of this century (IPCC 2007). This study contributes to the growing database of coastal

data, which is critical for use in the mitigation of ocean acidification at regional levels.

Literature Cited

Caldeira, K., M.E. Wickett. 2003. Anthropogenic carbon and ocean pH. *Nature*, 425: 365.

Carpenter, J.H. 1965. The accuracy of the Winkler method for dissolved oxygen analysis, *Limnology and Oceanography*, 10(1): 135 – 140.

Davenne, E. and D. Masson. 2001. Water properties in the Straits of Georgia and Juan de Fuca (British Columbia, Canada). Institute of Ocean Sciences, Sidney, BC: 1 – 41.

Dickson, A.G., C.L. Sabine, J.R. Christian. 2007. Guide to best practices for ocean CO_2 measurements. In: PICES Special Publication, 3, 191 pp.

Doney, S.C. 2010. The growing human footprint on coastal and open-ocean biogeochemistry. *Science*, 328: 1512 – 1516.

Doney, S.C., N. Mahowald, I. Lima, R.A. Feely, F.T. Mackenzie, J-F. Lamarque, P.J. Rasch. 2007. Impact of anthropogenic atmospheric nitrogen and sulfur deposition on ocean acidification and the inorganic carbon system. *Proceedings of the National Academy of Sciences*, 104(37): 14580 – 14585.

Doney, S.C., V.J. Fabry, R.A. Feely, J.A. Kleypas. 2009. Ocean acidification: the other CO2 problem. *Annual Reviews in Marine Science*, 1: 169 – 192.

Dumbauld, B.R., J.L. Ruesink, S.S. Rumrill. 2009. The ecological role of bivalve shellfish aquaculture in the estuarine environment: a review with application to oyster and clam culture in West Coast (USA) estuaries. *Aquaculture*, 290: 196 – 223.

Environment Canada. 2012. Fraser River Discharge Graph: http://www.wateroffice.ec.gc.ca/graph/realtimegraph_images/rtg.08MF005.3..2011-9-15.2011-12-10.000000.000000.....e.png. From 9 March 2012, Environment Canada Wateroffice.

Feely, R.A., C.L. Sabine, K. Lee, W. Berelson, J. Kleypas, V.J. Fabry, F.J. Millero. 2004. Impact of anthropogenic CO_2 on the $CaCO_3$ system in the oceans. *Science*, 305: 362 – 366.

Feely, R.A., C.L. Sabine, J.M. Hernandez-Ayon, D. Ianson, B. Hales. 2008. Evidence for upwelling of corrosive “acidified” water onto the continental shelf. *Science*, 320: 1490 – 1492.

Feely, R.A., S.C. Doney, S.R. Cooley. 2009. Ocean acidification: present conditions and future changes in a high-CO_2 world. *Oceanography*, 22(4): 35 – 47.

Feely, R.A., S.R. Alin, J. Newton, C.L. Sabine, M. Warner, A. Devol, C. Krembs, C. Maloy. 2010. The combined effects of ocean acidification, mixing, and

respiration on pH and carbonate saturation in an urbanized estuary. *Estuarine, Coastal and Shelf Science*, 88: 442 – 449.
Guinotte, J.M., V.J. Fabry. 2006. Ocean acidification and its potential effects on marine ecosystems. *Ann. N.Y. Acad. Sci.*, 1134: 320 – 342.
Hales, B., T. Takahashi, L. Bandstra. 2005. Atmospheric CO2 uptake by a coastal upwelling system. *Global Biogeochemical Cycles*, 19: 1 – 11.
Hauri, C., N. Gruber, G.-K. Plattner, S. Alin, R.A. Feely, B. Hales, PA. Wheeler. 2009. Ocean acidification in the California Current System. *Oceanography*, 22(4): 60 – 71.
Hoegh-Guldberg, O., J. Bruno. 2010. The impact of climate change on the world's marine ecosystems. *Science*, 328: 1523 – 1528.
Hofmann, G.E., J.E. Smith, K.S. Johnson, U. Send, L.A. Levin, F. Micheli, A. Paytan, N.N. Price, B. Peterson, Y. Yakeshita, P.G. Matson, E.D. Crook, K.J. Kroeker, M.C. Gambi, E.B. Rivest, C.A. Frieder, P.C. Yu, T.R. Martz. 2011. High-frequency dynamics of ocean pH: a multi-ecosystem comparison. *Plops ONE*, 6(12): 1 – 11.
Hopkinson, C.S., J.J. Vallino. 1995. The relationships among man's activities in watersheds and estuaries: a model of runoff effects on patterns of estuarine community metabolism. *Estuaries*, 18(4): 598 – 621.
Huppert, D.D., R.L Johnson, J. Leahy, K. Bell. 2003. Interactions between human communities and estuaries in the Pacific Northwest: trends and implications for management. *Estuaries*, 26(48): 994 – 1009.
Jackson, J.B.C., M.X. Kirby, W.H. Berger, K.A. Bjorndal, L.W. Botsford, B.J. Bourque, R.H. Bradbury, R. Cooke, J. Erlandson, J.A. Estes, T.P. Hughes, S. Kidwell, C.B. Lange, H.S. Lenihan, J.M. Pandolfi, C.H. Peterson, R.S. Steneck, M.J. Tegner, R.R. Warner. 2001. Historical overfishing and the recent collapse of coastal ecosystems. *Science*, 293(5530): 629 – 637.
Kelly et al. 2011. Mitigating local causes of ocean acidification with existing laws. *Science*, 332: 1036 – 1037.
Kelly, R.P. and M.R. Caldwell. 2012. Ten ways states can combat ocean acidification (and why they should). *Harvard Environmental Law Review*, Forthcoming.
Logan, C.A. 2010. A review of ocean acidification and America's response. *BioScience*, 60(10): 819 – 828.
Masson, D. 2002. Deep water renewal in the Strait of Georgia. *Estuarine, Coastal and Shelf Science*, 54: 115 – 126.
Mucci, A. 1983. The solubility of calcite and aragonite in seawater at various salinities, temperatures, and one atmosphere total pressure. *American Journal of Science*, 283: 780 – 799.
Orr, J.C., V.J. Fabry, O. Aumont, L. Bopp, S.C. Doney, R.A. Feely, A. Gnanadesikan, N. Gruber, A. Ishida, F. Joos, R.M. Key, K. Lindsay, R. Maier-Reimer, R. Matear, P. Monfray, A. Mouchet, R.G. Najjar, G-K. Plattner, K. B. Rodgers, C.L. Sabine, J.L. Sarmiento, R. Schlitzer, R.D. Slater, I.J. Totterdell, M-F. Weirig, Y. Yamanaka, A. Yool. 2005. Anthropogenic ocean acidification over the twenty-first century and its impact on calcifying organisms. *Nature*: 437: 681 – 686.

Redfield AC. 1950. Notes on the circulation of a deep estuary. Proceedings of the Colloquium on the Flushing of Estuaries. Woods Hole Oceanographic Institution.

Sabine, C.L., R.A. Feely, R.M. Key, J.L. Bullister, F.J. MIllero, K. Lee, T.-H. Peng, B. Tilbrook, T. Ono, C. S. Wong. 2007. Distribution of anthropogenic CO2 in the Pacific Ocean. *Global Biogeochemical Cycles*, 16(4): 1 – 17.

Salisbury, J., M. Green, C. Hunt, J. Campbell. 2008. Coastal acidification by rivers: a new threat to shellfish? *Eos*, 89(50): 513 – 528.

Simenstead, C.A., J.R. Cordell. 2000. Ecological assessment criteria for restoring anadromous salmonid habitat in Pacific Northwest estuaries. *Ecological Engineering*, 15: 283 – 302.

Van Geen, A., R.K. Takesue, J. Goddard, T. Takahashi, J.A. Barth, R.L. Smith. 2000. Carbon and nutrient dynamics during coastal upwelling off Cape Blanco, Oregon. *Deep-Sea Research II*, 47: 975 – 1002.

Winkler, L.W. 1888. Die Bestimmundges im Wassergelosten Sauerstoffes C.hem.Ber., 21: 2843-2855.

Chapter 2: Suggestions for Mitigation in Transboundary Regions

1. Introduction

1.1 Ocean Acidification

Ocean acidification is defined as, "…a reduction in the pH of the ocean over an extended period, typically decades or longer, which is caused primarily by uptake of carbon dioxide from the atmosphere, but can also be caused by other chemical additions or subtractions from the ocean" (IPCC 2011). Sources of chemical additions or subtractions from the ocean that contribute to acidification can be natural or anthropogenic in origin, and are not necessarily composed of carbon dioxide. The variability in the causes of ocean acidification makes it difficult to mitigate.

Natural sources of low pH inputs are variable throughout the year, and therefore can complicate mitigation efforts. Rivers have naturally low pH (Salisbury et al. 2008), so a pulse of discharge from a nearby river can cause a temporary decrease in pH. Eckman upwelling in eastern boundary current systems constitutes another natural input of low pH and high CO_2 waters to coastal areas (Hauri et al. 2009). Although the upwelled waters are lower in pH in part due to the ocean's absorption of anthropogenic CO_2 (Feely et al. 2010), the sources are not local and therefore cannot be mitigated locally.

Increasing nutrient levels and subsequent low levels of dissolved oxygen can exacerbate the effect of low pH on organisms. These inputs can be either anthropogenic or natural in origin. Low oxygen concentrations often are seasonal, and result from natural spring and fall blooms; however, anthropogenic activities also cause nutrient loads to increase. Anthropogenic sources of nutrients include runoff of fertilizer from agricultural areas and discharges from industrial activities (Diaz 2001). The lower oxygen levels can interact additively or synergistically to exacerbate the effects of low pH on organisms (Feely et. al. 2010).

Contributions to ocean acidification from sources other than carbon dioxide include sulfur oxides (SO_X) and nitrogen oxides (NO_X) that form acids in seawater (Doney et al. 2007). They can contribute to corrosive conditions in nearshore environments, especially those close to urban and industrialized centers. Consequently, the coastal zone is predicted to be at greater risk of impacts from ocean acidification due to the direct inputs of industrial SO_X and NO_X (Doney et al. 2007). These compounds can be in the form of air emissions from fossil fuel engines or in liquid effluents from industry. Point sources of liquid effluents include wastewater treatment plants, pulp and paper mills, mine effluent, and concentrated feedlot areas (Kelly and Caldwell 2012). Non-point sources include emissions from the shipping industry (Dalsøren et al.2008), fertilizer runoff, and runoff from impervious surfaces in urban areas.

1.1 Ocean Acidification in the Salish Sea

Regulation and reduction of SO_X and NO_X at local and regional scales could help to offset the effects of ocean acidification in some nearshore areas, especially in those where circulation is restricted, such as semi-enclosed bays and fjords. The waters of the Salish Sea are naturally low in pH and high in pCO_2 due to seasonal upwelling of corrosive water along Washington's outer coast and to natural respiration processes within Puget Sound (Feely et al. 2010). The addition of anthropogenic CO_2 from atmospheric sources intensifies corrosive conditions. As atmospheric additions of CO_2 continue throughout this century, waters of the Salish Sea will become increasingly corrosive, with the consequence that living marine organisms will be exposed to increasingly challenging environmental conditions. Throughout the Salish Sea, inputs of low-pH water come from a variety of land- and ocean- based sources in the U.S. and Canada. As a consequence, this transboundary region is likely to be vulnerable to the effects of ocean acidification.

Likely natural sources of low pH in this region are rivers, such as the Fraser River (British Columbia, Canada) and the Skagit River (Washington, U.S.), and intrusion of upwelled waters from the outer coast. Direct anthropogenic inputs come from major cities in the U.S. (Seattle, WA) and Canada (Vancouver and Victoria, B.C.), as well as industrial activity in each country.

2. History of U.S. and Canadian Transboundary Pollution

Local variation in OA is driven by Fraser River and other far-field sources, leading logically to the conclusion that efforts to buffer the influence of globally driven OA with local action must be transboundary in nature to be effective. The transboundary setting of this region increases complexities in regional mitigation strategies, but also offers opportunities to address the problem from a transboundary pollution perspective. Pollution issues between these two countries are not new. Indeed, the International Joint Commission (IJC) between the U.S. and Canada was established in 1909 to handle issues such as this. The IJC was established to target lake and river pollution along the international boundary. In 1991, the U.S.-Canada Air Quality Agreement was established to address air pollution issues. This Commission was successful in forming a bilateral agreement to reduce pollution in the Great Lakes, and a unilateral agreement to reduce air pollution from the U.S. to Canada (Hoberg 1991). Traditionally, the majority of transboundary pollution has resulted from U.S. pollution (Hsu and Parrish 2007; Duda 1994; Roelofs 1993; Hoberg 1991); however, the San Juan Archipelago is in an area in the U.S. that can receive ocean acidification pollution from Canada.

3. A Framework for Local Mitigation of Ocean Acidification in the Salish Sea

Waters in the Salish Sea already exhibit conditions consistent with ocean acidification (Feely et al. 2010). Consequently, actions to slow the rate of decline

in pH are called for. Established transboundary pollution agreements likely will need modification to address pollutants that contribute to and exacerbate ocean acidification. Here I propose an approach for addressing the issue (Figure 35). This approach utilizes scientific, geographic, and regulatory knowledge to provide a toolkit for regulators in the U.S. and Canada to advance mitigation strategies, without necessitating the creation of new transboundary agreements or policy instruments. Land use changes and increasing industrial outputs since the Industrial Revolution are primary causes of ocean acidification (Sabine et al. 2004). Although the problem of land use change and industrialization is global, their relative contributions vary at local and regional scales. Consequently, local- and regional-scale analysis is required for mitigation. In the transboundary region of the Salish Sea, fine-scale characterization of land use with respect to point-source inputs of nitrogen (NO_X) and sulfur (SO_X) oxide compounds can help to identify mitigation potential. While non-point sources of these contaminants are substantial (i.e., fossil fuel emissions), their regulation is inherently more difficult and is beyond the scope of local mitigation.

The first step in local mitigation is to create spatially explicit maps of the watersheds that contribute substantially to water quality in the transboundary region, inclusive of regions in the U.S. and Canada. Washington state (U.S.) and British Columbia (Canada) are the primary states and provinces involved; however, contributing watersheds could extend to Idaho and Oregon (U.S.) and Alberta (Canada).

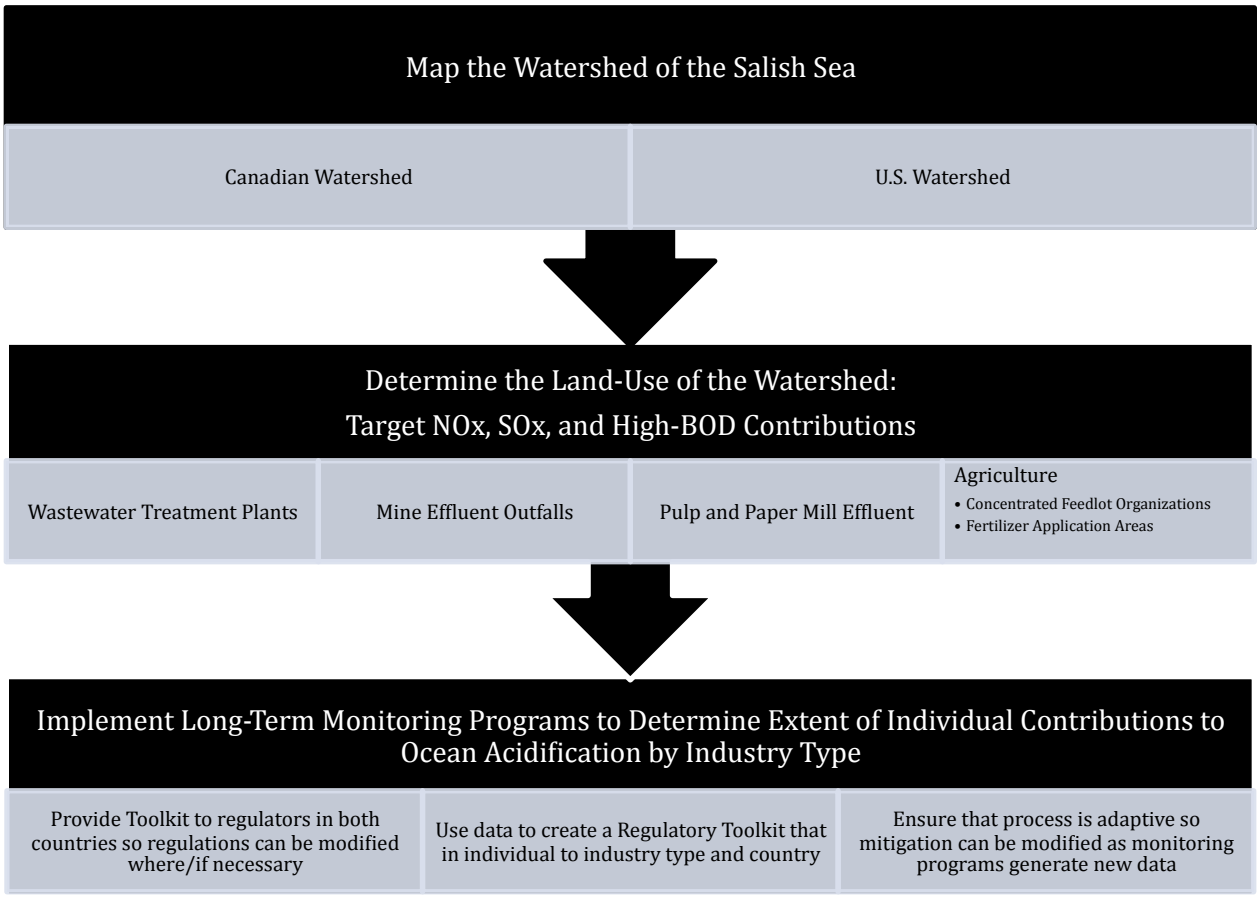

Figure 35. A framework for the development of mitigation tools to decrease the rate of ocean acidification.

Once identified, the magnitude of individual contributions of point sources can be determined. Long-term monitoring of point sources will allow determination of the magnitude of individual contributions to the local ocean acidification signal, in turn allowing modification of practices or application of technologies to reduce contributions.

Given sufficient characterization of regional conditions and inputs, policy recommendations can be formulated and presented in a 'toolkit.' This toolkit provides regulators with likelihood scenarios that can indicate the most significant causes of regional ocean acidification. Scenario building can help regulators to estimate the benefits of reducing inputs from individual sources, allowing regulators to target local and regional point sources for mitigation. Thus, the goal is to provide suggestions for action, instead of creating a treaty that could be time consuming and ineffective. Particular attention needs to be paid to the determination of the magnitude of pollution coming from each country so as to suggest specific, individualized mitigation tactics.

A crucial step in the preparation of this toolkit is to ensure that its design is adaptive. As long-term monitoring progresses, trends become apparent and changes can be detected, leading to adaptive modification of mitigation strategies. Annual review of monitoring data will allow detection of emergent trends and changes.

Policy solutions can be proposed following assessment of the appropriate environmental laws in each region. For the U.S., the Clean Water Act provides an appropriate regulatory instrument. In Canada, the Water Act of British Columbia can be reviewed for its utility in enforcing mitigation of sources that contribute to ocean acidification. Although the IJC is not intended for cases involving industrial sources of pollution, it could be useful in the framing of litigation.

4. Conclusion

The atmospheric carbon dioxide problem causing ocean acidification is global in nature, and thus is difficult to regulate. Local, non-carbon sources of ocean acidification could be easier to regulate than atmospheric sources of carbon dioxide because such sources typically fall under the regulatory authority of local and regional entities and agencies. Measuring non-carbon inputs from local sources will allow regulators to estimate relative contributions to the ocean acidification signal and the potential benefits of reducing such sources. An adaptive approach will allow tuning as conditions change. In a transboundary environment such as the Salish Sea, the approach presented here allows states on both sides of the boundary to respond in the most effective way possible, reducing regulatory burden while expediting mitigation.

Literature Cited

Dalsøren, S. B., M. S. Eide, Ø. Endresen, A. Mjelde, G. Gravir, I. S. A. Isaksen. 2008. Update on emissions and environmental impacts from the international fleet of ships. The contribution from major ship types and ports. *Atmospheric Chemistry and Physics Discussions*, 8: 18323 – 18384.

Diaz, R.J. 2001. Overview of hypoxia around the world. *Journal of Environmental Quality*, 30(2): 275 – 281.

Doney, S.C., N. Mahowald, I. Lima, R.A. Feely, F.T. Mackenzie, J-F. Lamarque, P.J. Rasch. 2007. Impact of anthropogenic atmospheric nitrogen and sulfur deposition on ocean acidification and the inorganic carbon system. *Proceedings of the National Academy of Sciences*, 104(37): 14580 – 14585.

Duda, A.M. 1994. Achieving pollution prevention goals for transboundary waters through International Joint Commission processes. *Water Science Technology*, 5: 223 – 231.

Feely, R.A., S.R. Alin, J. Newton, C.L. Sabine, M. Warner, A. Devol, C. Krembs, C. Maloy. 2010. The combined effects of ocean acidification, mixing, and respiration on pH and carbonate saturation in an urbanized estuary. *Estuarine, Coastal and Shelf Science*, 88: 442 – 449.

Hauri, C., N. Gruber, G.-K. Plattner, S. Alin, R.A. Feely, B. Hales, PA. Wheeler. 2009. Ocean acidification in the California Current System. *Oceanography*, 22(4): 60 – 71.

Hoberg, G. 1991. Sleeping with an elephant: the American influence on Canadian environmental regulation. *Journal of Public Policy*, 11(1): 107 – 131.

Hsu, S.-L., A.L. Parrish. 2007. Canada-US transboundary harm: international environmental lawmaking and the threat of extraterritorial reciprocity. *Virginia Journal of International Law*, 48(1): 1 – 64.

IPCC 2011: Workshop report of the Intergovernmental Panel of Climate Change Workshop on Impacts of Ocean Acidification on Marine Biology and Ecosystems [Field, C.B., V. Barros, T.F. Stocker, D. Qin, K.J. Mach, G.-K. Plattner, M.D. Mastrandrea, M. Tignor and K.L. Ebi (eds.)]. IPCC Working Group II Technical Support Unit, Carnegie Institution, Stanford, California, United States of America, pp.164.

IPCC. 2007. Climate change 2007: synthesis report. Pp 1 – 52.

Kelly, R.P. and M.R. Caldwell. 2012. Ten ways states can combat ocean acidification (and why they should). *Harvard Environmental Law Review*, Forthcoming.

Parrish, A.L. 2005. Trail smelter déjà vu: extraterritoriality, international environmental law, and the search for solutions to Canadian-US transboundary water pollution disputes. *Boston University Law Review*, 85(355): 363 – 428.

Roelofs, J.L. 1993. United States-Canada air quality agreement: a framework for addressing transboundary air pollution problems. *Cornell International Law Journal*, 26: 421 – 454.

Salisbury, J., M. Green, C. Hunt, J. Campbell. 2008. Coastal acidification by rivers: a new threat to shellfish? *Eos*, 89(50): 513 – 528.

Sabine, C.L., R.A. Feely, N. Gruber, R.M. Key, K. Lee, J.L. Bullister, R. Wanninkhof, C.S. Wong, D.W.R. Wallace, B. Tilbrook, F.J. Millero, T.-H. Peng, A. Kozyr, T. Ono, A.F. Rios. 2004. The oceanic sink for anthropogenic CO2. *Science*, 305 (5682): 367 – 371.